Specific interaction between Group B *Streptococcus*

CC17 hypervirulent clone and phagocytes

Anne-Sophie Bourrel[1,2,×], Amandine Picart[1,×], Jose-Carlos Fernandez[1], Constantin Hays[1,2], Bruno Saubamea[4], Virginie Mignon[4], Claire Poyart[1,2,3], Asmaa Tazi[1,2,3]Julie Guignot[1*]

[1]Université de Paris, Institut Cochin, INSERM, U1016, CNRS, UMR8104, F-75014 Paris, France; [2]Hôpitaux Universitaires Paris Centre, Cochin, Assistance Publique Hôpitaux de Paris, France; [3]Centre National de Référence des Streptocoques, France;

[4] IFR71-IMTCE, Plateau technique Imagerie Cellulaire & Moléculaire;

[×] These authors contributed equally to this work

***** To whom correspondence should be addressed: julie.guignot@inserm.fr

ORCID number: 0000-0001-8890-4028. Tel: + 33 1 40 51 64 13; Fax: + 33 1 40 51 64 54.

Institut Cochin, 22 rue Méchain 75014 Paris, France.

CONFLICT OF INTEREST:

The authors have declared that no conflict of interest exists.

KEYWORDS: CC17, *Streptococcus agalactiae*, Group B Streptococcus, phagocytosis, THP-1.

Abbreviations: CC17 (complex clonal 17), GBS (group B Streptococcus).

SUMMARY

Streptococcus agalactiae also named Group B *Streptococcus* (GBS) is the most significant pathogen causing invasive infections, such as bacteremia and meningitis in neonates. Worldwide epidemiological studies have shown that a particular clonal complex (CC) of capsular serotype III, the CC17, is strongly associated with meningitis in neonates and is therefore designated as the hypervirulent clone. Macrophages are a permissive niche for intracellular bacteria of all GBS clones. In this study we deciphered the specific interaction of GBS CC17 strains with macrophages. Our study reveals that CC17 strains are phagocytosed at a higher rate than GBS non-CC17 strains by human monocytes and macrophages in cellular models and primary cells. CC17 hyper-phagocytosis is preceded by an initial hyper-attachment step to macrophages mediated by the PI-2b pilus (Spb1) and the CC17 specific HvgA surface protein. We showed that two different inhibitors of scavenger receptors (fucoidan and poly(I)) specifically inhibited CC17 phagocytosis while they did not affect non-CC17 phagocytosis. Once phagocytosed, both CC17 and non-CC17 strains remain in a LAMP-1 positive vacuole that ultimately fuses with lysosomes, and their survival within macrophages is similar. Bothe strains display a basal egress which occurs independently from actin and microtubules networks. Our findings provide new insights into the interplay between the hypervirulent GBS CC17 and major players of host innate immune response. This enhanced phagocytosis could reflect a peculiar capacity of CC17 lineage to subvert the host immune defense and establish a niche for intracellular persistence.

INTRODUCTION

The innate immune system plays a crucial role during host's interaction with pathogens, particularly in neonates who exhibit a naive adaptive immune system and are more vulnerable to invasive infections (1). Innate immunity largely relies on professional phagocytic cells, including macrophages, monocytes, dendritic cells, as well as granulocytic cell types such as neutrophils, which constitute the first line of defense against pathogens. Phagocytosis is defined as a cellular uptake pathway for particles larger than 0.5 µm in diameter, including foreign substances, apoptotic cells and microorganisms. The phagocytic process is initiated upon recognition of specific pathogen-associated molecular patterns (PAMPs) by pattern recognition receptors (PRRs). The intracellular signaling cascades triggered upon phagocytosis lead to actin polymerization which generates membrane protrusions required for bacterial engulfment, the activation of phagosome maturation leading to microbial killing, and the production of pro-inflammatory mediators that orchestrate the initiation of adaptive immunity. Signal transduction during phagocytosis is specific to the cell type and to the receptor(s) involved, and can impact the intracellular fate of the microorganism (2). Professional phagocytes express a large number of surface phagocytic receptors which are divided into opsonic or non-opsonic receptors. Opsonic phagocytic receptors include the Fc receptors and complement receptors, which recognize antibody- or complement-opsonized pathogens, but also some non-opsonized pathogens (3, 4). Non-opsonic receptors are constituted by a wide array of family receptors including integrins, C-type lectins or scavenger receptors that directly interact with PAMPs. Once internalized, the pathogen resides in a distinct organelle called the phagosome which rapidly undergoes maturation by a series of fusion and fission events with endocytic organelles, and acquires numerous proteins such as the late endosome/lysosome-associated membrane proteins LAMP-1 and LAMP-2. Ultimately, the phagosome fuses with lysosomes to become a phagolysosome with microbicidal features including a very acidic lumen (pH ~ 4.5), lysosomal proteases, and reactive oxygen species (ROS).

Streptococcus agalactiae, also named Group B *Streptococcus* (GBS), is a capsulated chain-forming Gram-positive coccus commonly found in the gut and the lower urogenital tract of approx. 20% healthy adults (5). Although rarely pathogenic in adults, GBS is the leading cause of invasive infection in neonates (6). Two neonatal GBS-associated syndromes, referred to as "early-onset disease" (EOD) and "late-onset disease" (LOD), have been described, depending on the age at onset. EOD occurs during the first week of life and is the result of a vertical mother-to-neonate transmission prior to or during parturition. EOD often manifests by respiratory distress that rapidly progresses into sepsis and less frequently meningitis. In contrast, LOD, which occurs from 7 days to 3 months of age, could result from a vertical transmission during delivery but also from horizontal contamination after birth linked to nursing, healthcare or breast

feeding (7). LOD manifests as a bacteremia highly associated to meningitis (20-50% cases) and the first pathophysiological step is presumed to be an asymptomatic colonization of the infant gastrointestinal tract allowing subsequent seeding of the bloodstream and penetration of the blood–brain barrier (7, 8). Based on the capsular polysaccharide composition, GBS has been classified into 10 distinct serotypes (Ia, Ib, and II–IX). Serotype III is the most frequently identified serotype in young infants (48.9%) (9). More specifically, within serotype III, multilocus sequence typing (MLST) has identified a hypervirulent lineage termed clonal complex 17 (CC17) which accounts for a substantial proportion of EOD cases (25%) and the majority of LOD cases (70%) worldwide, whereas it is isolated in about 13% of non-pregnancy-related adult infections and colonization (7, 10, 11). GBS CC17 is a highly successful invasive clone strongly associated with neonatal meningitis (12-14) that harbors a number of specific genes encoding two surface proteins named Srr2 and HvgA involved in the crossing of the intestinal and blood brain barriers (8, 15-17). Although not totally exclusive to the CC17 lineage, the pilus islands PI-2b encoding the Spb1 adhesin is also found in the vast majority of CC17 strains, while rarely expressed in others human lineages (15, 18).

GBS has developed several mechanisms to resist immune detection, phagocytosis and microbial degradation (19). The capsular polysaccharide (CPS) is one of the major virulence factors of GBS allowing evasion from the host immune system, notably by preventing host complement deposition on the bacterial surface (20), (21). Although capsule limits phagocytosis of complement-opsonized GBS, it is well described that serum or complement opsonized-GBS can be phagocytosed by Fc and complement receptors respectively (19, 22). However, there are large gaps in our understanding of the phagocytosis of non-opsonized GBS. The persistence of GBS in macrophages relies on numerous bacterial factors (19). Interestingly, non-opsonized uptake leads to a better survival within phagocytes (19, 23-25). However, the receptor(s) and signaling pathway(s) involved in non-opsonized GBS phagocytosis are unknown. In addition, the expression of some virulence factors associated to the CC17 lineage such as Spb1 have been described to increase phagocytosis (26-28). However, the capacity of CC17 lineage to exhibit enhanced phagocytosis and survival in macrophages compared to those of other GBS lineage is still disputed (25, 29 , 30 , 31).

In the present study, we used a collection of GBS isolates representing a range of capsule types and Sequence Types (ST) and showed that CC17 strains are more phagocytosed than non-CC17 isolates and that the hyper-phagocytosis is due to an increased initial adhesion to phagocytes. Once internalized, GBS CC17 and non-CC17 do not differentially affect the phagolysosome maturation and their ability to survive within phagocytes is similar. Altogether, the enhanced phagocytosis of GBS CC17 could reflect a peculiar

capacity of the hypervirulent lineage to subvert the host immune defense and establish a niche for intracellular persistence.

RESULTS

GBS CC17 strains are more phagocytosed by macrophages and monocytes

The literature shows conflicting results on GBS lineages capacity to be phagocytosed (25, 29 , 30 , 31). Therefore, we performed a phagocytosis assay using THP-1 differentiated macrophages to compare the phagocytosis level of a relevant collection of GBS isolates responsible for human invasive infections including 27 CC17 strains and 40 non–CC17 strains (Table S2). Our results show that CC17 strains are more phagocytosed than non-CC17 strains (2.3-fold increased) (Fig. 1A). We next used two well-characterized and fully sequenced GBS strains of CC17 (strain BM110) and CC23 (strain NEM316) to characterize the lineage-differences and the phagocytosis process, and confirmed the hyper-phagocytosis of GBS CC17 in THP-1 macrophages (Fig. 1B), in primary human monocytes derived macrophages (hMDM) (Fig. 1C), in non-differentiated THP-1 monocytes (Fig. 1D), and in primary human monocytes (Fig. 1E).

Since the capsule is a major bacterial factor in GBS phagocytosis, we analyzed its contribution to the hyper-phagocytosis phenotype of GBS CC17. First, we stratified the results of the phagocytosis assay performed with the clinical GBS strains presented in Fig. 1A according to their capsular type. CC17 strains being almost exclusively of capsular type III and more rarely of type IV, we distinguished within CC17 and non-CC17 isolates those of capsular type III, IV and all the other types, and found that CC17 strains hyper-phagocytosis was independent from the capsular type (Fig. S1A). To confirm this result, we analyzed the phagocytosis level of BM110 (CC17) and NEM316 (non-CC17) mutants inactivated for capsule expression. As expected, an increased phagocytosis of capsule deficient strains was observed (Fig. S1B). Nevertheless, the increased phagocytosis of the CC17 isolate compared to the non-CC17 isolate could still be observed with the corresponding non-capsulated mutants (Fig. S1B).

Altogether, these results show that CC17 strains are more phagocytosed than non-CC17 strains in a capsule independent manner.

CC17 hyper-phagocytosis is preceded by a hyper-adhesion step

Phagocytosis can result from the direct recognition of phagocytic receptor(s) by the bacteria or be preceded by the recognition of receptor(s) allowing a primary adhesion step to phagocytic cells. Therefore, we analyzed the adhesion of GBS clinical strains to THP-1 macrophage and show that CC17 strains exhibit higher adhesion than non-CC17 strains (1.9-fold increased) (Fig. 2A, Table S2). The increased adhesion of CC17 isolates was not related to the capsular serotype (Fig. S2A) and was still observed in the absence of capsule expression (Fig. S2B). The hyper-adhesion of the well described CC17 isolate BM110 compared to the non-CC17 isolate NEM316 to THP-1 macrophages (Fig.2B) was also observed with THP-1 monocytes

(Fig. 2C) and hMDM (Fig. 2D).

HvgA and Spb1 promote CC17's adhesion and phagocytosis

This observation prompted us to search for CC17 specific virulence factors that may account for this hyper-adhesion and hyper-phagocytosis phenotypes. To this end, we tested the phagocytosis of BM110 (CC17 strain) mutated in genes encoding CC17 specific (Srr2, HvgA) or highly associated (Spb1) virulence factors (15). Using THP-1 macrophages, both Δ*hvgA* and Δ*spb1* mutants exhibited reduced adhesion (23% and 48% reduction, respectively) and phagocytosis (65% and 54% reduction, respectively) compared to the wild-type, in contrast to the Δ*srr2* mutant (Fig. 3A and B respectively). The role of Spb1 in GBS phagocytosis has already been described (26, 27, 32), but not that of HvgA. To confirm the direct involvement of the HvgA surface protein in phagocytosis, we used a close relative, non-pathogenic, and non-adherent *Lactococcus lactis*, in which an expression vector encoding *hvgA* and enabling its expression at the bacterial surface was introduced (16). Using THP-1 macrophages, the heterologous expression of HvgA in *L. lactis* led to a significant 2-fold increase in adhesion (Fig. 3C) and to a 3-fold increase in phagocytosis compared to *L. lactis* carrying an empty vector (Fig. 3D). The involvement of HvgA in CC17 adhesion and phagocytosis was also observed using hMDM (Fig. 3E and F, respectively).

Signal transduction leading to phagocytosis is similar between CC17 and non-CC17 strains

To gain further insight into these findings, Scanning Electron Microscopy (SEM) was used to characterize the early contact between GBS and macrophages. In agreement with our results (Fig. 2B), SEM revealed that 15 minutes after infection, many BM110 (CC17) chains have adhered to macrophages while fewer NEM316 (non-CC17) chains were found adherent (Fig. 4A, left panel). In addition, uptake of BM110 (CC17) was accompanied by the formation of filopodia-like cellular protrusions which were rarely observed in the case of NEM316 (non-CC17) (Fig. 2B) or BM110Δ*hvgA* (not shown). The direct contribution of HvgA to this phenotype was further confirmed using the HvgA-expressing *L. lactis* isolate which induced, in contrast to the non-HvgA-expressing isolate, numerous filopodia-like structures by THP-1 macrophages (Fig. 4B).

Cell membrane protrusion formation leading to phagocytosis results from cytoskeleton rearrangements, which are mediated by specific signaling cascades induced by bacterial binding to cell surface receptors (33). Numerous signaling molecules regulate the cytoskeleton, including the small Rho GTPases Rho, Rac and CDC42 known to allow the formation of actin stress fibers, lamellipodial protrusions, and filopodia, respectively (34). To better characterize the molecular pathways involved in GBS CC17 phagocytosis, we performed phagocytosis assays using a wide array of inhibitors targeting different signaling molecules

(Table S3). We found that BM110 (CC17) phagocytosis was inhibited by cytochalasin D, ZCL278, staurosporine, wortmannin, LY29002 and PP2 indicating that CC17 phagocytosis required actin, the small GTPse CDC42, as well as different kinases (PKC, Pi3K and Src), respectively. In contrast, microtubules, the small GTPase Rac and the kinases Syk and Rock were not involved (Fig. 5A and Table S3). Interestingly, we found that NEM316 (non-CC17) phagocytosis involved similar signaling molecules than BM110 (CC17 strain) (Fig. 5B).

Altogether, our results show that while only CC17 bacteria are captured by numerous filopodia, due to the presence of HvgA, similar signaling molecules are involved in CC17 and non-CC17 phagocytosis (33).

CC17 uptake in macrophages is inhibited by scavenger receptor inhibitors

Phagocytes express multiple receptors involved in the initial adhesion and phagocytosis of bacteria. To identify the precise nature of the macrophage receptor(s) involved in GBS phagocytosis, GBS CC17 phagocytosis was evaluated in cells pre-treated with various blocking molecules targeting putative receptor(s) (Table S3). Whereas the inhibitors targeting FCyR, complement receptors, integrins and lectin receptors did not affect GBS CC17 phagocytosis, fucoidan and poly(I), two different scavenger receptor inhibitors, significantly reduced it by 60% and 32%, respectively (Fig. 6A). Importantly, the inactive analog of poly(I), poly(C), used as a negative control, had no effect on CC17 phagocytosis (Fig. 6A). Interestingly, these phenotypes were specific to CC17 strain since no reduction of NEM316 (non-CC17) phagocytosis was observed using these 2 scavenger receptor inhibitors (Fig. 6B). This result indicates that some scavenger receptors can contribute to a significant proportion of GBS CC17 entry into macrophages.

Scavenger receptors constitute a large family of membrane-associated pattern recognition receptors (PRRs) that act as phagocytic receptors mediating direct non-opsonic adhesion and uptake of pathogenic microbes and/or their products (35). To determine which scavenger receptor(s) contribute to the internalization of GBS CC17 in THP-1 macrophages, we characterized by RT-PCR the expression profile of scavenger receptors in THP-1 macrophages and, given that the hyper-phagocytosis of GBS CC17 is conserved in hMDM and monocytes, we extended the analysis of scavenger receptors expression profile to these cell types (Fig. 6C). Using the recent classification of scavenger receptors (36), we identified that, out of the 25 different scavenger receptors tested, 13 were shared by our 3 cellular models (Fig. 6C). Next, we silenced the expression of each of these 13 individual scavenger receptors by siRNA to address their involvement in GBS CC17 uptake. Efficient knockdown levels were confirmed on 2 individual genes expressed by THP-1 macrophages for which the knockdown efficiency was 78 and 98 % (Fig. S3A). As an additional control, the silencing of the complement receptor impaired the phagocytosis of complemented-

red blood cells (96% decreased) (Fig. S3B), demonstrating that siRNA in THP-1 macrophages was efficient. However, when individual scavenger receptors were silenced, no significant reduction in BM110 (CC17) uptake was observed (Fig. 6D). Last, in agreement with the phagocytosis assays using phagocytosis receptors inhibitors, BM110 (CC17 strain) phagocytosis was not decreased in THP-1 macrophages silenced for FCyR, complement receptors, α5 or β3 integrin expression, or for Plaur or CD44 (Fig. S3C).

CC17 and non-CC17 strains display similar capacity to survive within macrophages

After phagocytosis, the phagocytic vacuole containing the bacteria undergoes maturation events leading to the formation of a phagolysosome required for efficient bacterial degradation. GBS is known to be able to survive within macrophages for up to24 hours (24-26, 30, 31). We therefore compared the intracellular fate of GBS strains in in THP-1 macrophages. The maturation of phagosomes containing GFP-expressing BM110 (CC17) and GFP-NEM316 (non-CC17) (Table S1) was followed by fluorescence microscopy at various time-points after phagocytosis (t=0, t=2h30 and t=5h). BM110 bacteria colocalizing with LAMP-1 and with the Lysotracker (a fluorescent dye labeling acidic organelles such as phagolysosome) were quantified after immunofluorescence staining (Fig. 7A and C). No statistical differences were observed in the kinetic of phagosome maturation between BM110 (CC17) and NEM316 (non-CC17) whatever the time-point (Fig. 7B and D), indicating that the delivery of GBS CC17 and non-CC17 to late endosomes or lysosomes is similar. Besides, the survival ability of GBS clinical isolates (10 CC17 and 17 non-CC17 strains) was compared by quantifying intracellular viable bacteria. To avoid a bias due to the higher-phagocytosis of CC17 strains compared to non-CC17 strains, survival results were normalized for each GBS strain to the number of initially phagocytosed bacteria. No significant difference was observed in the survival abilities of CC17 and non-CC17 strains (Fig. 7E), whatever the capsular type (Fig. S4). Consistently, HvgA and Spb1 were not involved in CC17 survival within THP-1 macrophages (Fig. 7F) or hMDM (Fig. 7G).

Taken together, these results revealed that the intracellular fate of GBS CC17 and non-CC17 after phagocytosis is similar.

CC17 and non-CC17 strains can escape macrophages by a non-active phenomenon

In order to gain insight into the physiological relevance of our study, we analyzed the capacity of GBS strains to escape THP-1 macrophages. After phagocytosis and antibiotic treatment to eliminate extracellular bacteria, cells were washed extensively to get rid of antibiotics and then further incubated for a short period of time (45min and 1h30) to allow potential bacterial escape without any bacterial multiplication within the extracellular media. GBS egress normalized to the percentage of initial

phagocytosis showed that BM110 (CC17) and NEM316 (non-CC17) strains displayed similar capacity to escape from macrophages (Fig. 8A). GBS egress from THP-1 macrophages was neither inhibited by cytochalasin D nor by nocodazole (Fig. 8B), indicating that it is independent of actin cytoskeleton and microtubules, respectively. This suggests that bacterial escape does not result from the recycling of the bacteria-containing vacuole to the plasma membrane. Macrophage lysis induced by GBS infection was therefore tested. However, no LDH release differences were observed between infected and non-infected macrophages (Fig. 8C). This indicate that GBS egress is likely due to spontaneous macrophage lysis.

DISCUSSION

The innate immune response is critical for pathogen clearance, especially in neonates in whom the adaptive immune system is not yet fully mature and the specific antibodies required for adaptive immune response are usually lacking. Phagocytic cells populate all tissues and organs of the body where they play an important role in pathogen clearance. However, numerous pathogens have evolved sophisticated strategies to avoid capture and/or killing by phagocytes. By expressing multiple bacterial factors involved in acid stress response and ROS resistance, including the orange carotenoid pigment hemolysin, the glutathione or the superoxide dismutase (SodA), GBS has been shown to efficiently survive within phagocytes (37). This capacity to avoid killing by phagocytes is thought to allow the establishment of a survival niche that could contribute to bacterial persistence within tissues. However, although some GBS lineages display specific virulence traits, their ability to induce specific responses during their interaction with phagocytes remains controversial. In a study performed by Rogers et al. using 35 isolates from various GBS lineages, no significant differences were observed in the phagocytosis of GBS strains stratified by capsular serotype or MLST (29). In contrast, a study performed with a more discrete number of GBS isolates (15 GBS strains including 4 CC17 strains) found that CC17 are phagocytosed by macrophages at significantly higher rates than other GBS isolates (31). Our study, performed with a higher number of invasive GBS clinical isolates (27 CC17 isolates and 40 non-CC17 isolates) demonstrates that GBS CC17 strains are more phagocytosed than non-CC17 strains. These discrepancies may be attributed to the use by Rogers et al. of heat-inactivated GBS which could have denatured bacterial surface proteins involved in phagocytosis. In agreement with this hypothesis, we demonstrated that the hyper-phagocytosis of CC17 strains does not depend on the polysaccharidic capsule`, a major GBS virulence factor which protects the bacteria from phagocytosis but, rather on the expression of the surface proteins Spb1, the backbone protein of the PI-2b pilus, and the HvgA adhesin.

In contrast, we did not observe any role for the Srr2 surface protein in GBS CC17 uptake by macrophages. Yet, Srr2 was previously described as being involved in CC17 phagocytosis (28). Genome sequencing of the Srr2 mutant generated by Six et al. revealed a phage insertion in a putative coding region compared to the parental wild-type strain. However, no spurious mutations or phages mobility have been observed in the Srr2 mutant used in this study and more recently by our group (8, 17). Although the consequence of such phage insertion in the Srr2 mutant strain constructed by Six et al. has not been investigated, it might account for this discrepancy. Moreover, we and others have found that blocking the known Srr2-receptors, α5β1 and αvβ3 integrins, by mimetic peptides (RGD and/or RGfV) or by silencing α5 or β3 integrin expression does not affect CC17 phagocytosis (this study and (23)). Together, these data are consistent

and indicate that the Srr2 surface protein is not involved in phagocytosis.

The Spb1 protein is the backbone protein of the PI-2b pilus which is expressed by the vast majority of CC17 strains and by a few non-CC17 stains (38). We showed that both SpB1 and HvgA contribute to GBS CC17 hyper-phagocytosis by mediating a high level of initial adhesion. In addition of being involved in adhesion, HvgA expression seems to be important to trigger the formation of numerous filopodia like structures allowing the capture of CC17 bacteria by macrophages. Filopodia formation is known to require the Cdc42 GTPase activity leading to actin polymerization (34). Accordingly, we found that CC17 phagocytosis was strongly dependent on actin and Cdc42. However, and surprisingly, while filopodia were rarely observed around non-CC17 bacteria, we found that CC17 and non-CC17 strains efficient internalization within phagocytes required similar signalling molecules, including Cdc42. This could reflect the recognition of similar cellular receptors by CC17 and non-CC17 strains with different affinities. Such phenomenon has previously been described for GBS interaction with fibrinogen which exhibits 10-fold higher affinity for CC17 strains than for non-CC17 strains (39).

The search for cellular receptor(s) involved in the non-opsonized phagocytosis of GBS has been investigated by many teams (22, 23, 40). Despite the efforts, the receptor(s) involved in the non-opsonized phagocytosis of GBS are still unknown. Our study indicates that FCyRs, complement receptors and CD14 are not involved in the phagocytosis of non-opsonized GBS, as also described previously (22, 23, 40). Accordingly, GBS phagocytosis is independent of Syk and Rock kinases that are known to be involved in FCyR and complement receptor signalling, respectively (41). Interestingly, fucoidan and poly(I), two broad scavenger receptor inhibitors reduced the phagocytosis of CC17 strain, while having a non-significant effect on the phagocytosis of a non-CC17 strains. Macrophage scavenger receptors are a diverse family of proteins that recognized polyanionic ligands and can act as PRR involved in the recognition of various microbial ligands (42). The polynucleotide ligand poly(I) acts by efficient competitive inhibition of the binding of other polyanionic ligands to the cationic collagenous binding domain of some scavenger receptors. Similarly, fucoidan, which are abundant sulfated polysaccharides found in brown algae, easily interact with positively charged molecules because of their high negative charge at neutral pH (43, 44). These molecules have been successfully used to inhibit adhesion and/or phagocytosis of several pathogens (45, 46). The inhibitory effect of fucoidan and poly(I) on CC17 phagocytosis led us to conclude that scavenger receptor(s) might be involved in the adhesion and/or uptake of non-opsonized CC17 bacteria by macrophages. Interestingly, it has been recently described that the scavenger receptor SSC4D interacts with BM110 (CC17 strain) (47). SSCD4 is a secreted scavenger receptor rendering this molecule unlikely involved in the initial adherence of CC17 bacteria to the macrophage surface. Accordingly, in our model,

we have confirmed that silencing SSC4D expression does not affect CC17 phagocytosis (not shown). Despite our efforts, the siRNA screen performed to identify potential scavenger receptor(s) involved in GBS uptake was unsuccessful. Several hypotheses could explain this failure. Because CC17 hyper-phagocytosis is a phenotype conserved between macrophages and monocytes from cell lines and donors, we hypothesized that the receptor(s) involved in CC17 hyper-phagocytosis is also conserved in these different cell type. However, we cannot exclude the possibility that different scavenger receptors in each cellular model allow CC17 uptake, or that several scavenger receptors might have a cooperative effect. Also, as described, the list of scavenger receptors is constantly growing, and we might have missed the scavenger receptor involved in GBS CC17 phagocytosis. Finally, we cannot exclude a non-specific effect of fucoidan and poly(I), or an indirect effect of these inhibitors on the signaling of others PRRs, as described previously (48).

The capacity of CC17 strains to survive within macrophages compared to non CC17 strains have been controversial (25, 26, 30, 31). We found that CC17 and non-CC17 strains display similar intracellular fate with similar survival capacity. In agreement with this result, we found that Sbp1 and HvgA proteins do not contribute to intracellular survival. As CC17 strains display higher phagocytosis level, the discrepancies between the different studies likely come from the fact that intracellular survival ability should be determined using the initial number of intracellular bacteria rather than the initial bacterial inoculum. While displaying similar capacity to survive and escape from macrophages, the higher initial load of intracellular CC17 might *in fine* lead to a higher number of surviving and eventually released bacteria. This latest is of fundamental importance as intracellular survival and bacterial egress could contribute to bacterial persistence and dissemination. Moreover, specific interactions between CC17 and macrophages may elicit variable cytokine expression profiles and signaling pathways (49), potentially inducing different phagocytes behavior. In conclusion, the specific traits associated to CC17 lineage interactions with phagocytes likely contribute to their particular virulence and to the pathophysiology of infection.

MATERIAL AND METHODS

Bacterial strains

Bacterial strains used in this study are listed in Table S1. GBS BM110 and NEM316 are well characterized capsular serotype III strains isolated from blood cultures of neonates (16). GBS strain BM110, an CC17/ST17, was used as reference strain for CC17 strains, while GBS NEM316, an CC23/ST23, was used as reference strain for non-CC17 strains. Other GBS clinical strains isolated from invasive infections (i.e. from blood culture, cerebrospinal fluid or other sterile sites) were obtained from the French National Reference Center for Streptococci in Paris (http://www.cnr-strep.fr) which performed capsular serotyping and MLST for each clinical GBS strains (Table S2). All bacterial strains were cultured in Todd Hewitt (TH) broth or agar (Difco Laboratories, Detroit, MI) at 37°C, except for *L. lactis* which was grown at 30°C. When necessary, antibiotics were used to maintain plasmids at the following concentrations, spectinomycin 100 µg ml^{-1}, erythromycin 100 µg ml^{-1}.

THP-1 cell line and culture conditions

THP-1 (TIB-202 from ATCC) cell line is a spontaneous immortalized monocyte-like cell line, derived from the peripheral blood of a childhood case of acute monocytic leukemia. THP-1 cells were cultured at 37°C under a 5% CO_2 atmosphere in RPMI1640 + Glutamax (Gibco), 10% Fetal Calf Serum (FCS, Gibco) and 0.05 mM β-mercapto-ethanol. Cells were passaged twice per week and kept at a cell concentration below 1×10^6 cells /mL. THP-1 cell line was routinely tested for mycoplasma contamination (Mycoalert mycoplasma detection kit, LONZA). To differentiate monocytic THP-1 into adherent macrophages, cells were seeded in 24-well plates at 3×10^5 cells per well in culture media containing 200 nM phorbol 12-myristate 13-acetate (PMA) during 3 days, then media was replaced by fresh RPMI1640 complete media without PMA for 5 more days.

Isolation and culture of primary human Peripheral Blood Mononuclear Cells (PBMCs) and Monocytes-Derived Macrophages (hMDMs)

Blood of adult healthy donors was used (Etablissement Français du Sang, Ile de France, Site Saint-Antoine-le Crozatier) with the appropriate ethics prior approval as stated in the EFS/ Inserm agreement #18EFS030, ensuring that all donors gave a written informed consent and providing anonymized samples. Primary human monocytes were negatively selected using the EasySep Human Monocyte enrichment kit (StemCell®) following the manufacturer's instructions. For hMDM, primary human PBMCs were isolated by density gradient sedimentation in Histopaque® (Sigma) according to the manufacturer's

recommendations. Monocytes were then selected by adhesion to dishes for 2 h at 37°C in FCS-free medium (RPMI 1640 medium supplemented with 0.1 mg/ml gentamicin. Monocytes were differentiated into hMDMs for at least 7 days in complete medium containing 10 ng/mL of recombinant human macrophage colony-stimulating factor (rhM-CSF; R&D systems).

Phagocytosis and survival assay in monocyte and macrophages

Monocytes and macrophages from THP-1 cell line and primary cells were used to study the phagocytosis and/or the intracellular survival of GBS strains. All experiments were carried out with GBS strain grown to mid-log phase and washed twice with sterile Phosphate buffer saline (PBS) before infection. After addition of bacteria, a quick centrifugation (5 min, 200 × g) was performed to synchronize infection. Phagocytes were infected for 45 min with GBS strains, using a multiplicity of infection (MOI) of 10 bacteria per cell, at 37°C and under a 5% CO_2 atmosphere in RPMI 1640 medium. After 1 h or 45 minutes of infection for monocytes or macrophages, respectively, phagocytes were washed 3 times with PBS. Remaining extracellular bacteria were killed using RPMI 1640 medium supplemented with Penicillin G / Streptomycin (100 units/ml / 0.1 mg/ml) and Gentamicin (0.2 mg/ml) at 37°C and 5% CO_2. After antibiotics treatment to kill extracellular bacteria, cells were washed twice and either lysed directly to evaluate phagocytosis or further incubate in RPMI1640 medium without any antibiotic to follow intracellular survival before being lysed. Phagocytes were lysed using sterile ice-cold water and serial dilutions of the lysates were plated onto TH agar for colony forming units (CFU) counting. The percent of phagocytosis was calculated as follows: (CFU on plate count / CFU in inoculum) × 100. The percent of survival was calculated as follows: (CFU on plate count / CFU phagocytosed) × 100. When specified, results were expressed as normalized to the control strain (BM110). Assays were performed in triplicate and were repeated at least three times.

Adhesion assay onto monocytes and macrophages

For adhesion assays, infection was performed as described for phagocytosis but at 4°C and with ice-cold RPMI1640 medium to avoid engulfment of bacteria. After 3 washes with PBS to remove non-adherent bacteria, phagocytes were lysed and CFU were determined as described for phagocytosis. The percent of adhesion was calculated as follows: (CFU on plate count / CFU in inoculum) × 100. When specified, results were expressed as normalized to the control strain. Assays were performed in triplicate and were repeated at least three times.

Phagocytosis assay in presence of inhibitors/reagents

Selected compounds were tested for their ability to block GBS phagocytosis. All inhibitors and reagents used in this study are listed in Table S3. THP-1 macrophages were pretreated with inhibitors/reagents for 1 h prior infection with BM110 or NEM316 strains. Inhibitors/reagents were left during the time of infection at the same concentration. Treatments did not affect bacterial or cell viability (assessed by Lactate dehydrogenase cytotoxicity kit®, Promega, according to the manufacturer's instructions) (data not shown). The percent of phagocytosis was calculated as follows: (CFU on plate count / CFU in inoculum) × 100 and results were normalized to untreated condition.

Evaluation of bacterial egress from macrophages

To assess bacterial escape from macrophages, supernatants were recovered from phagocytosis assays after an additional 30 min step without any antibiotic to enable bacteria to escape in the extracellular medium. The percent of bacterial escape was calculated as follows: (CFU on plate count / CFU phagocytosed) × 100.

RNA extraction, cDNA synthesis and RT-PCR

RNAs were extracted from non-infected THP-1 macrophages, monocyte and hMDM using the NucleoSpin® RNA kit (Macherey-Nagel®) according to the manufacturer's instructions. RNA concentration was determined using a NanoDrop 2000 spectrophotometer. Then, 1 µg RNA were reverse- transcribed into cDNA using the SuperScript® IV Reverse Transcription Kit (Invitrogen), following manufacturer's instructions. PCR were carried out with Green Taq DNA polymerase (Promega) on cDNA using primers described in Table S4 (Table S4). Primers were designed in order to amplify all variants of targeted receptor(s). Amplification products were resolved in 1% (w/v) agarose gel.

siRNA transfection

To silence the expression of putative phagocytic receptors, pools of three or four siRNA duplexes (Dharmacon) were used. The silencer select negative control-1 siRNA (Ambion) was used as negative control. THP-1 were seeded in twenty-four-well plates for 24 h in presence of 200 nM of PMA then transfected with 50 nM siRNA using Lipofectamine RNAIMAX (Invitrogen) according to the manufacturer's instructions and incubated for a further 3 days. Efficiency of knockdown was assessed by Western Blot analysis on 2 independent targets.

Immunofluorescent staining and image analysis

To follow intracellular fate of bacterial strains, THP-1 macrophages were infected for 45 minutes as described for phagocytosis then washed extensively and fixed at different time point post-phagocytosis

(0, 2h30 or 5 h) on glass coverslips with 4% paraformaldehyde (PFA) for 10 min then washed with PBS. Following fixation, samples were permeabilized and saturated with P/S buffer containing 0.2% saponin and 10% serum in PBS for 1h at room temperature, then incubated for at least 1 h at room temperature with the primary antibody LAMP1 (DSHB H4A3) diluted in P/S buffer. After 3 washes with PBS, samples were incubated for 1 h at room temperature with conjugated-secondary's antibodies (Jackson ImmunoResearch Laboratories) diluted in P/S buffer. DAPI was used to counter-stain nuclei.

To enable detection of acidic compartments (phagolysosome), THP-1 macrophages were incubated 30 minutes before the end of infection with Lysotracker red DND-99 (Invitrogen) at a final concentration of 75 nM, fixed with 4% PFA for 10 min, then washed with PBS and processes for DAPI staining.

After 3 washes in PBS, coverslips were mounted in DAKO fluorescent mounting media (DAKO). Image acquisitions were realized using confocal laser scanning microscopy (Leica DMI6000) coupled to a spinning disk confocal head (YokogawaCSU-X1M1), controlled by the Metamorph 7.7.5 software (Cochin Institute's microscopy facility, IMAG'IC). Images were processed using the ImageJ software. At least 300 cells were analyzed for each sample in four independent experiments.

Electron Microscopy

All incubations were performed at room temperature except when otherwise indicated. Macrophages grown on glass coverslips were infected as described previously then, fixed in 0.1M sodium cacodylate buffer, pH 7.4 containing 2.5% glutaraldehyde and 1% PFA for 60 min. After washing in cacodylate buffer (2x10 min), cells were fixed in 1% OsO_4 diluted in cacodylate buffer for 45 min at 4°C. After washing in cacodylate buffer (2x10 min), samples were dehydrated in an ascending series of ethanol (30%, 50%, 70%, 95%, 100%, 100%, 100% - 10 min each), followed by Hexamethyldisilazane (HMDS)/ethanol (1/1) for 10 min and HMDS for 10 min. After overnight air drying, each coverslip was placed on a double-sided sticky tape on the top of an aluminum stub and sputter coated with Au/Pd. Images were acquired using a Jeol LV6510 (Jeol, Croissy-sur-Seine, France).

Statistical analysis

All assays were performed at least in four independent experiments. Data represent mean ± SEM and statistical analyses were performed using GraphPad Prism 5.0 (GraphPad Software, San Diego, California). Significance levels were set at $*p \leq 0.05$; $**p \leq 0.01$;$***p \leq 0.001$.

AUTHOR CONTRIBUTIONS

JG designed the research. ASB, AP, JCF, CH and JG performed the experiments. ASB, AP, JG analyzed the data. BS and VM performed electron microscopy experiments. AF, AT, CP provided intellectual input and guidance. JG wrote the manuscript and ASB, AF, AT, CP contributed to finalizing the manuscript. All authors discussed results and reviewed the final version of the manuscript.

ACKNOWLEDGMENTS

We are grateful to Glen Ulett for the gift of the GFP plasmid. We thank Cristina Candeias for technical assistance, Shaynoor Dramsi for BM110Δ*spb1* and NEM316Δ*cps* mutant strains and the Imag'IC core facility of the Cochin Institute.

FINANCIAL SUPPORT

This work was supported by Agence Nationale de la Recherche (ANR) (Grant StrepB2brain, ANR-17-CE15-0026-01). ASB was a doctoral fellow funded by Université de Paris Cité.

REFERENCES

1. Marodi L. 2006. Neonatal innate immunity to infectious agents. Infect Immun 74:1999-2006.
2. Rosales C, Uribe-Querol E. 2017. Phagocytosis: A Fundamental Process in Immunity. Biomed Res Int 2017:9042851.
3. Mittal R, Sukumaran SK, Selvaraj SK, Wooster DG, Babu MM, Schreiber AD, Verbeek JS, Prasadarao NV. 2010. Fcgamma receptor I alpha chain (CD64) expression in macrophages is critical for the onset of meningitis by Escherichia coli K1. PLoS Pathog 6:e1001203.
4. Orrskog S, Rounioja S, Spadafina T, Gallotta M, Norman M, Hentrich K, Falker S, Ygberg-Eriksson S, Hasenberg M, Johansson B, Uotila LM, Gahmberg CG, Barocchi M, Gunzer M, Normark S, Henriques-Normark B. 2013. Pilus adhesin RrgA interacts with complement receptor 3, thereby affecting macrophage function and systemic pneumococcal disease. MBio 4:e00535-12.
5. Patras KA, Nizet V. 2018. Group B Streptococcal Maternal Colonization and Neonatal Disease: Molecular Mechanisms and Preventative Approaches. Front Pediatr 6:27.
6. Seale AC, Bianchi-Jassir F, Russell NJ, Kohli-Lynch M, Tann CJ, Hall J, Madrid L, Blencowe H, Cousens S, Baker CJ, Bartlett L, Cutland C, Gravett MG, Heath PT, Ip M, Le Doare K, Madhi SA, Rubens CE, Saha SK, Schrag SJ, Sobanjo-Ter Meulen A, Vekemans J, Lawn JE. 2017. Estimates of the Burden of Group B Streptococcal Disease Worldwide for Pregnant Women, Stillbirths, and Children. Clin Infect Dis 65:S200-S219.
7. Tazi A, Plainvert C, Anselem O, Ballon M, Marcou V, Seco A, El Alaoui F, Joubrel C, El Helali N, Falloukh E, Frigo A, Raymond J, Trieu-Cuot P, Branger C, Le Monnier A, Azria E, Ancel PY, Jarreau PH, Mandelbrot L, Goffinet F, Poyart C. 2019. Risk Factors for Infant Colonization by Hypervirulent CC17 Group B Streptococcus: Toward the Understanding of Late-onset Disease. Clin Infect Dis doi:ciz033 [pii] 10.1093/cid/ciz033 5427769 [pii].
8. Hays C, Touak G, Bouaboud A, Fouet A, Guignot J, Poyart C, Tazi A. 2019. Perinatal hormones favor CC17 group B Streptococcus intestinal translocation through M cells and hypervirulence in neonates. Elife 8.
9. Edmond KM, Kortsalioudaki C, Scott S, Schrag SJ, Zaidi AK, Cousens S, Heath PT. 2012. Group B streptococcal disease in infants aged younger than 3 months: systematic review and meta-analysis. Lancet 379:547-56.
10. Joubrel C, Tazi A, Six A, Dmytruk N, Touak G, Bidet P, Raymond J, Trieu Cuot P, Fouet A, Kerneis S, Poyart C. 2015. Group B streptococcus neonatal invasive infections, France 2007-2012. Clin Microbiol Infect 21:910-6.
11. Vuillemin X, Hays C, Plainvert C, Dmytruk N, Louis M, Touak G, Saint-Pierre B, Adoux L, Letourneur F, Frigo A, Poyart C, Tazi A. 2021. Invasive group B Streptococcus infections in non-pregnant adults: a retrospective study, France, 2007-2019. Clin Microbiol Infect 27:129 e1-129 e4.
12. Manning SD, Springman AC, Lehotzky E, Lewis MA, Whittam TS, Davies HD. 2009. Multilocus sequence types associated with neonatal group B streptococcal sepsis and meningitis in Canada. J Clin Microbiol 47:1143-8.
13. Teatero S, McGeer A, Low DE, Li A, Demczuk W, Martin I, Fittipaldi N. 2014. Characterization of invasive group B streptococcus strains from the greater Toronto area, Canada. J Clin Microbiol 52:1441-7.
14. van Kassel M, de Boer G, Teeri S, Jamrozy D, Bentley S, Brouwer M, Van der Ende A, Van de Beek D, Bijlsma M. 2021. Molecular epidemiology and mortality of group B streptococcal meningitis and infant sepsis in the Netherlands: a 30-year nationwide surveillance study. The lancet microbe 2.

15. Brochet M, Couve E, Zouine M, Vallaeys T, Rusniok C, Lamy MC, Buchrieser C, Trieu-Cuot P, Kunst F, Poyart C, Glaser P. 2006. Genomic diversity and evolution within the species Streptococcus agalactiae. Microbes Infect 8:1227-43.
16. Tazi A, Disson O, Bellais S, Bouaboud A, Dmytruk N, Dramsi S, Mistou MY, Khun H, Mechler C, Tardieux I, Trieu-Cuot P, Lecuit M, Poyart C. 2010. The surface protein HvgA mediates group B streptococcus hypervirulence and meningeal tropism in neonates. J Exp Med 207:2313-22.
17. Deshayes de Cambronne R, Fouet A, Picart A, Bourrel AS, Anjou C, Bouvier G, Candeias C, Bouaboud A, Costa L, Boulay AC, Cohen-Salmon M, Plu I, Rambaud C, Faurobert E, Albiges-Rizo C, Tazi A, Poyart C, Guignot J. 2021. CC17 group B Streptococcus exploits integrins for neonatal meningitis development. J Clin Invest 131.
18. Springman AC, Lacher DW, Wu G, Milton N, Whittam TS, Davies HD, Manning SD. 2009. Selection, recombination, and virulence gene diversity among group B streptococcal genotypes. J Bacteriol 191:5419-27.
19. Korir ML, Manning SD, Davies HD. 2017. Intrinsic Maturational Neonatal Immune Deficiencies and Susceptibility to Group B Streptococcus Infection. Clin Microbiol Rev 30:973-989.
20. Chang YC, Nizet V. 2020. Siglecs at the Host-Pathogen Interface. Adv Exp Med Biol 1204:197-214.
21. Marques MB, Kasper DL, Pangburn MK, Wessels MR. 1992. Prevention of C3 deposition by capsular polysaccharide is a virulence mechanism of type III group B streptococci. Infect Immun 60:3986-93.
22. Henneke P, Takeuchi O, Malley R, Lien E, Ingalls RR, Freeman MW, Mayadas T, Nizet V, Akira S, Kasper DL, Golenbock DT. 2002. Cellular activation, phagocytosis, and bactericidal activity against group B streptococcus involve parallel myeloid differentiation factor 88-dependent and independent signaling pathways. J Immunol 169:3970-7.
23. Valentin-Weigand P, Benkel P, Rohde M, Chhatwal GS. 1996. Entry and intracellular survival of group B streptococci in J774 macrophages. Infect Immun 64:2467-73.
24. Cornacchione P, Scaringi L, Fettucciari K, Rosati E, Sabatini R, Orefici G, von Hunolstein C, Modesti A, Modica A, Minelli F, Marconi P. 1998. Group B streptococci persist inside macrophages. Immunology 93:86-95.
25. Cumley NJ, Smith LM, Anthony M, May RC. 2012. The CovS/CovR acid response regulator is required for intracellular survival of group B Streptococcus in macrophages. Infect Immun 80:1650-61.
26. Chattopadhyay D, Carey AJ, Caliot E, Webb RI, Layton JR, Wang Y, Bohnsack JF, Adderson EE, Ulett GC. 2011. Phylogenetic lineage and pilus protein Spb1/SAN1518 affect opsonin-independent phagocytosis and intracellular survival of Group B Streptococcus. Microbes Infect 13:369-82.
27. Perichon B, Guignot J, Szili N, Gao C, Poyart C, Trieu-Cuot P, Dramsi S. 2019. Insights into Streptococcus agalactiae PI-2b pilus biosynthesis and role in adherence to host cells. Microbes Infect 21:99-103.
28. Six A, Bellais S, Bouaboud A, Fouet A, Gabriel C, Tazi A, Dramsi S, Trieu-Cuot P, Poyart C. 2015. Srr2, a multifaceted adhesin expressed by ST-17 hypervirulent Group B Streptococcus involved in binding to both fibrinogen and plasminogen. Mol Microbiol 97:1209-22.
29. Rogers LM, Gaddy JA, Manning SD, Aronoff DM. 2018. Variation in Macrophage Phagocytosis of Streptococcus agalactiae Does Not Reflect Bacterial Capsular Serotype, Multilocus Sequence Type, or Association with Invasive Infection. Pathog Immun 3:63-71.
30. Korir ML, Laut C, Rogers LM, Plemmons JA, Aronoff DM, Manning SD. 2017. Differing mechanisms of surviving phagosomal stress among group B Streptococcus strains of varying genotypes. Virulence 8:924-937.

31. Flaherty RA, Aronoff DM, Gaddy JA, Petroff MG, Manning SD. 2021. Distinct Group B Streptococcus Sequence and Capsule Types Differentially Impact Macrophage Stress and Inflammatory Signaling Responses. Infect Immun 89.
32. Perichon B, Szili N, du Merle L, Rosinski-Chupin I, Gominet M, Bellais S, Poyart C, Trieu-Cuot P, Dramsi S. 2017. Regulation of PI-2b Pilus Expression in Hypervirulent Streptococcus agalactiae ST-17 BM110. PLoS One 12:e0169840.
33. Uribe-Querol E, Rosales C. 2020. Phagocytosis: Our Current Understanding of a Universal Biological Process. Front Immunol 11:1066.
34. Krugmann S, Jordens I, Gevaert K, Driessens M, Vandekerckhove J, Hall A. 2001. Cdc42 induces filopodia by promoting the formation of an IRSp53:Mena complex. Curr Biol 11:1645-55.
35. Pombinho R, Sousa S, Cabanes D. 2018. Scavenger Receptors: Promiscuous Players during Microbial Pathogenesis. Crit Rev Microbiol 44:685-700.
36. PrabhuDas MR, Baldwin CL, Bollyky PL, Bowdish DME, Drickamer K, Febbraio M, Herz J, Kobzik L, Krieger M, Loike J, McVicker B, Means TK, Moestrup SK, Post SR, Sawamura T, Silverstein S, Speth RC, Telfer JC, Thiele GM, Wang XY, Wright SD, El Khoury J. 2017. A Consensus Definitive Classification of Scavenger Receptors and Their Roles in Health and Disease. J Immunol 198:3775-3789.
37. Shabayek S, Spellerberg B. 2017. Acid Stress Response Mechanisms of Group B Streptococci. Front Cell Infect Microbiol 7:395.
38. Lu B, Wang D, Zhou H, Zhu F, Li D, Zhang S, Shi Y, Cui Y, Huang L, Wu H. 2015. Distribution of pilus islands and alpha-like protein genes of group B Streptococcus colonized in pregnant women in Beijing, China. Eur J Clin Microbiol Infect Dis 34:1173-9.
39. Seo HS, Minasov G, Seepersaud R, Doran KS, Dubrovska I, Shuvalova L, Anderson WF, Iverson TM, Sullam PM. 2013. Characterization of fibrinogen binding by glycoproteins Srr1 and Srr2 of Streptococcus agalactiae. J Biol Chem 288:35982-96.
40. Albanyan EA, Vallejo JG, Smith CW, Edwards MS. 2000. Nonopsonic binding of type III Group B Streptococci to human neutrophils induces interleukin-8 release mediated by the p38 mitogen-activated protein kinase pathway. Infect Immun 68:2053-60.
41. Lee HJ, Woo Y, Hahn TW, Jung YM, Jung YJ. 2020. Formation and Maturation of the Phagosome: A Key Mechanism in Innate Immunity against Intracellular Bacterial Infection. Microorganisms 8.
42. Taban Q, Mumtaz PT, Masoodi KZ, Haq E, Ahmad SM. 2022. Scavenger receptors in host defense: from functional aspects to mode of action. Cell Commun Signal 20:2.
43. Lin Z, Tan X, Zhang Y, Li F, Luo P, Liu H. 2020. Molecular Targets and Related Biologic Activities of Fucoidan: A Review. Mar Drugs 18.
44. Sigola LB, Fuentes AL, Millis LM, Vapenik J, Murira A. 2016. Effects of Toll-like receptor ligands on RAW 264.7 macrophage morphology and zymosan phagocytosis. Tissue Cell 48:389-96.
45. Baba M, Snoeck R, Pauwels R, de Clercq E. 1988. Sulfated polysaccharides are potent and selective inhibitors of various enveloped viruses, including herpes simplex virus, cytomegalovirus, vesicular stomatitis virus, and human immunodeficiency virus. Antimicrob Agents Chemother 32:1742-5.
46. Thelen T, Hao Y, Medeiros AI, Curtis JL, Serezani CH, Kobzik L, Harris LH, Aronoff DM. 2010. The class A scavenger receptor, macrophage receptor with collagenous structure, is the major phagocytic receptor for Clostridium sordellii expressed by human decidual macrophages. J Immunol 185:4328-35.
47. Cardoso MS, Santos RF, Almeida S, Sa M, Perez-Cabezas B, Oliveira L, Tavares J, Carmo AM. 2021. Physical Interactions With Bacteria and Protozoan Parasites Establish the Scavenger Receptor SSC4D as a Broad-Spectrum Pattern Recognition Receptor. Front Immunol 12:760770.

48. Dutot M, Grassin-Delyle S, Salvator H, Brollo M, Rat P, Fagon R, Naline E, Devillier P. 2019. A marine-sourced fucoidan solution inhibits Toll-like-receptor-3-induced cytokine release by human bronchial epithelial cells. Int J Biol Macromol 130:429-436.
49. Musser JM, Mattingly SJ, Quentin R, Goudeau A, Selander RK. 1989. Identification of a high-virulence clone of type III Streptococcus agalactiae (group B Streptococcus) causing invasive neonatal disease. Proc Natl Acad Sci U S A 86:4731-5.
50. Xia FD, Mallet A, Caliot E, Gao C, Trieu-Cuot P, Dramsi S. 2015. Capsular polysaccharide of Group B Streptococcus mediates biofilm formation in the presence of human plasma. Microbes Infect 17:71-76.

FIGURES LEGENDS

Figure 1: CC17 GBS strains are more phagocytosed by monocytes and macrophages than non-CC17 GBS strains. Phagocytosis level of GBS strains was assessed by CFU counting after 45 min of infection at MOI 10 followed by 1h antibiotic treatment to kill extracellular bacteria using THP-1 cell line (A, B, D), hMDM primary cells (C) or human primary monocytes (E). Phagocytes were infected either with CC17 and non-CC17 GBS clinical isolates from invasive infections, each point representing a clinical strain (A) or with GBS strains BM110 (CC17) and NEM316 (non-CC17) (B, C, D, E). Results are expressed as the percentage of phagocytosis relative to BM110 strain phagocytosis with red horizontal lines indicating mean value (A) or to the initial inoculum (B, C, D, E). Statistical analysis: data shown are mean ± SEM of at least four independent experiments. t test (A) or Mann Whitney test (B, C, D, E) were performed with NS, non-significant; *, $p < 0.05$; **, $p < 0.01$; ***, $p < 0.001$.

Figure 2: CC17 GBS strains are more adherent to phagocytes than non-CC17 strains. Adhesion level of GBS strains was assessed after one hour of infection at MOI 10, and at 4°C to avoid bacterial engulfment, by CFU counting using THP-1 cell line (A, B, C) or hMDM primary cells (D). Phagocytes were infected either with CC17 and non-CC17 GBS clinical isolates isolated from invasive infections, each point representing a clinical strain (A) or with GBS strains BM110 (CC17) and NEM316 (non-CC17) (B, C, D). Results are expressed as the percentage of adherent bacteria relative to the adhesion level of BM110 strain with the red horizontal lines indicating mean value (A) or to the initial inoculum (B, C, D). Statistical analysis: data shown are mean ± SEM of at least four independent experiments. Mann Whitney test (B, C, D) or t test (A) were performed with NS, non-significant; *, $p < 0.05$; **, $p < 0.01$; ***, $p < 0.001$.

Figure 3: HvgA surface protein and Spb1 pilus protein are involved in CC17's hyper-adhesion and phagocytosis. Adhesion (A, C, E) and phagocytosis (B, D, F) levels were assessed using THP-1 macrophages cell line (A, B, C, D) or hMDM primary cells (E, F). Macrophages were infected with BM110 (CC17 strain) and its derivative mutated strains (BM110Δ*srr2*, BM110Δ*hvgA* or BM110Δ*spb1* (A, B, E, F), or with *Lactococcus lactis* strain carrying an empty vector (*L;lactis* + vector) or a vector expressing HvgA protein (*L. lactis* +HvgA) (C, D). Results are expressed as relative level compared to BM110 strain (A-F). Statistical analysis: data shown are mean ± SEM of at least four independent experiments. Kruskall Wallis test followed by Dunn's multiple comparisons tests (A, B), and Mann Whitney test (C, D, E, F), were performed, with NS, non-significant; *, $p < 0.05$; **, $p < 0.01$; ***, $p < 0.001$.

Fig 4: CC17 bacteria are captured by filopodia. Scanning electron microscopy (SEM) micrographs of THP-1 macrophages infected for 15 min (A) or 30 min (B). (A and B, left panel). Micrographs showing bacterial adherence to macrophages cell surface. Boxed areas correspond to magnification of insets (right panel) showing the capture of BM110 (CC17 strain) and *Lactococcus lactis* expressing HvgA (*L. lactis* +HvgA) by filopodia (arrows), while very few filopodia were observed for NEM316 and *L. lactis* strains.

Fig 5: Signal transduction leading to phagocytosis is similar for CC17 and non-CC17 strains. Phagocytosis of BM110 (CC17 strain) (A) or NEM316 (non-CC17 strain) (B) were assessed by CFU counting after 45 min of infection at MOI 10 followed by 1h antibiotic treatment to kill extracellular bacteria using THP-1 macrophages. Cells were pre-treated for one-hour prior infection with cytochalasinD, ZCL178, staurosporin, wortmannin, LY29002, PP2, nocodazole, NSC23766, BAY61-3606 and Y27632 to inhibit actin polymerization, CDC42, protein kinase C, PI3kinase, Pi3kinase, Src kinase, microtubule polymerization, Rac, Syc and Rock, respectively. Results are expressed as the percentage of phagocytosis relative to untreated condition. Statistical analysis: data shown are mean ± SEM of at least four independent experiments. One-Way ANOVA with Dunnett multiple comparisons test were performed with NS, non-significant; *, $p < 0.05$; **, $p < 0.01$; ***, $p < 0.001$.

Fig 6: Scavenger receptors inhibitors leads to a decreased phagocytosis level of CC17 GBS in macrophages. (A, B, D) Phagocytosis level in THP-1 macrophages was assessed by CFU counting after 45 min of infection at MOI 10 with GBS strain BM110 (CC17 strain) (A, D) or NEM16 (non-CC17 strain) (B). followed by 1h antibiotic treatment to kill extracellular bacteria. (A) Macrophages were pre-treated 1h before infection to block FCγ receptors (Fc Block™), complement receptor 3 (CR3 blocking antibody), lectin receptors (mannose, mannan, laminarin), integrins receptors (RGD and RGDfV mimetic peptides), or (A, B) scavenger receptors inhibitors (Fucoidan and poly(I) or inactive analog poly(C). (C) Expression of scavenger receptors genes was assessed by RT-PCR using THP-1 macrophages, THP-1 monocyte and hMDM cDNA. Actin and VE-cadherin gene expression was used as positive and negative controls of expression, respectively. Genomic DNA (gDNA) was used to validate primers efficiency. (D) Involvement of scavenger receptors on BM110 (CC17 strain) phagocytosis was assessed by silencing scavenger receptors expression by si-RNA screening. Results are expressed as the percentage of phagocytosis relative to the untreated control condition (A, B) or to the scramble control condition (D). Statistical analysis: data shown are mean ± SEM of at least four independent experiments. Kruskall Wallis test followed by Dunn's multiple

comparisons tests were performed (A, B, D), with NS, non-significant; *, $p < 0.05$; **, $p < 0.01$; ***, $p < 0.001$.

Figure 7: CC17 and non-CC17 GBS strains exhibit similar intracellular fate. Intracellular fate of BM110 (CC17) and NEM316 (non-CC17) strains was followed by microscopy (A, D) or CFU count (E, F, G) in THP-1 macrophages (A, F) or hMDM (G). (A, C) Representative confocal microscopy images of THP-1 macrophages infected with BM110-GFP (CC17 strain) (green) and labelled with anti-LAMP1 antibody (red) (A) or Lysotracker® (red) (B). Boxed areas correspond to magnification of insets. Dotted lines indicate cell perimeters. Scale bar: 5 µm. (B, D) Quantification of bacteria associated with LAMP1 (B) or Lysotracker® (D) was performed after 0, 2h30 or 5 h post-phagocytosis. Results are expressed as the percentage of bacteria positive for LAMP1 (B) or Lysotracker® (D) staining. (E, F, G) Percentage of survival was assessed by CFU counting of viable bacteria 2h30 after phagocytosis. (E) Macrophages were infected with CC17 and non-CC17 GBS clinical isolates from invasive infections, each point representing a clinical strain or (F, G) with the BM110 (CC17) strain and its derivative mutated strains (BM110Δ*hvgA* or BM110Δ*spb1*). Results are expressed as the percentage of viable intracellular bacteria normalized to the initial phagocytosis level intracellular load. Statistical analysis: data shown are mean ± SEM of at least four independent experiments. (E) Two-way ANOVA (A), Tuckey multiple comparison (B, D) and Mann Whitney (E, F, G) tests were performed with NS, non-significant; *, $p < 0.05$; **, $p < 0.01$; ***, $p < 0.001$.

Fig 8: GBS strains can escape macrophages independently of actin and microtubules. GBS egress from THP-1 macrophages was assessed by CFU counting. THP-1 were infected for 45 min or 1h30 at MOI 10 with GBS strains, then treated with antibiotic to kill extracellular bacteria. Bacterial egress was measured for BM110 (CC17) or NEM316 (non-CC17) strains in absence of any treatment (A) or in the presence of actin (cytochalasin D) or microtubules (nocodazole) depolymerizing agents added after phagocytosis (B). Results are expressed as the percentage of viable bacteria release in the cell supernatants normalized to the number of phagocytosed bacteria (A, B). Cell lysis during bacterial egress was measured by evaluating LDH release (C). Statistical analysis: data shown are mean ± SEM of at least four independent experiments. Two-way Anova with Bonferroni post-test (A) Kruskall Wallis (B) and one-Way ANOVA with Dunnett's post-tests were performed with NS, non-significant; *, $p < 0.05$; **, $p < 0.01$; ***, $p < 0.001$.

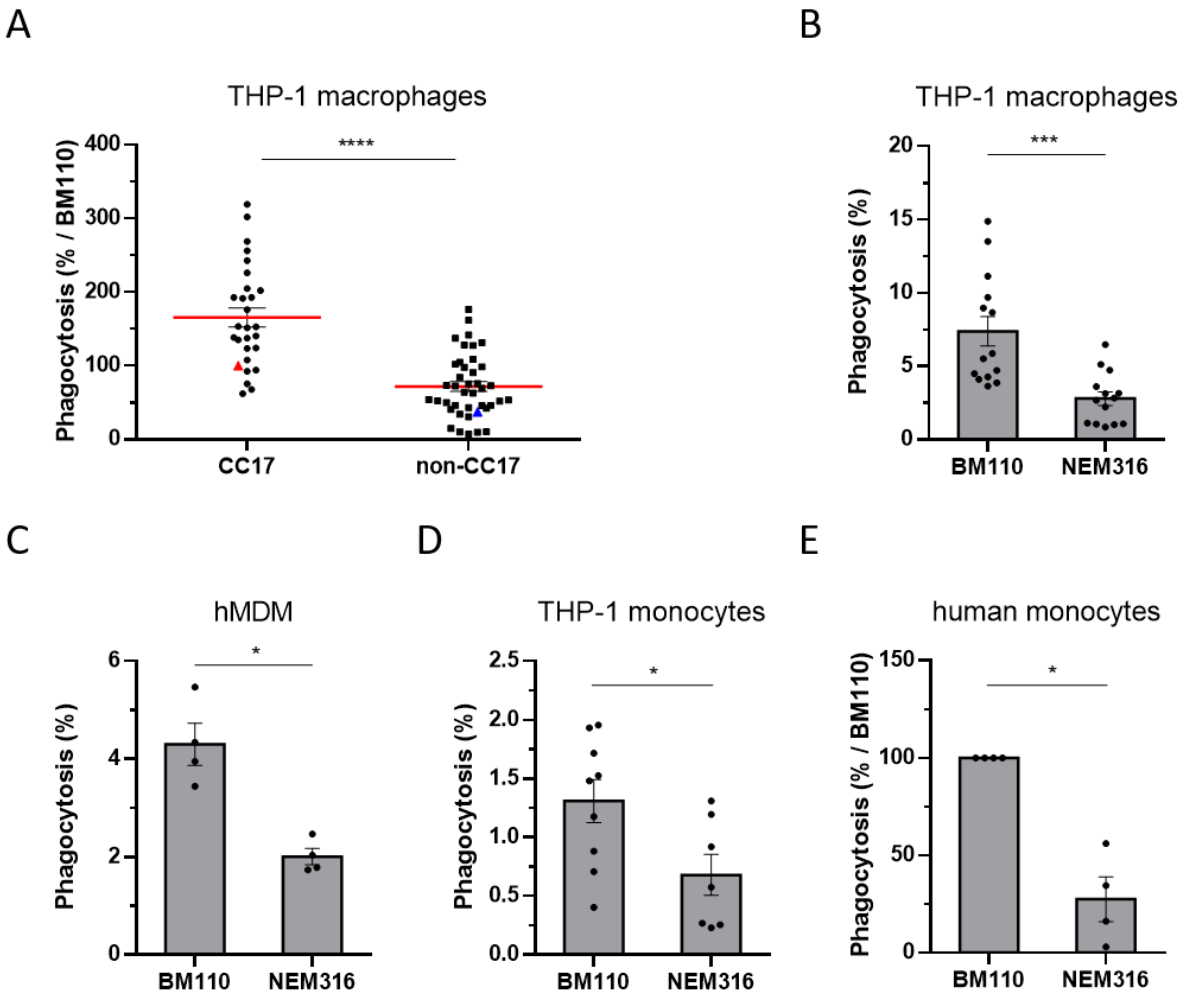

Figure 1: CC17 GBS strains are more phagocytosed by monocytes and macrophages than non-CC17 GBS strains. Phagocytosis level of GBS strains was assessed by CFU counting after 45 min of infection at MOI 10 followed by 1h antibiotic treatment to kill extracellular bacteria using THP-1 cell line (A, B, D), hMDM primary cells (C) or human primary monocytes (E). Phagocytes were infected either with CC17 and non-CC17 GBS clinical isolates from invasive infections, each point representing a clinical strain (A) or with GBS strains BM110 (CC17) and NEM316 (non-CC17) (B, C, D, E). Results are expressed as the percentage of phagocytosis relative to BM110 strain phagocytosis with red horizontal lines indicating mean value (A) or to the initial inoculum (B, C, D, E). Statistical analysis: data shown are mean ± SEM of at least four independent experiments. t test (A) or Mann Whitney test (B, C, D, E) were performed with NS, non-significant; *, $p < 0.05$; **, $p < 0.01$; ***, $p < 0.001$.

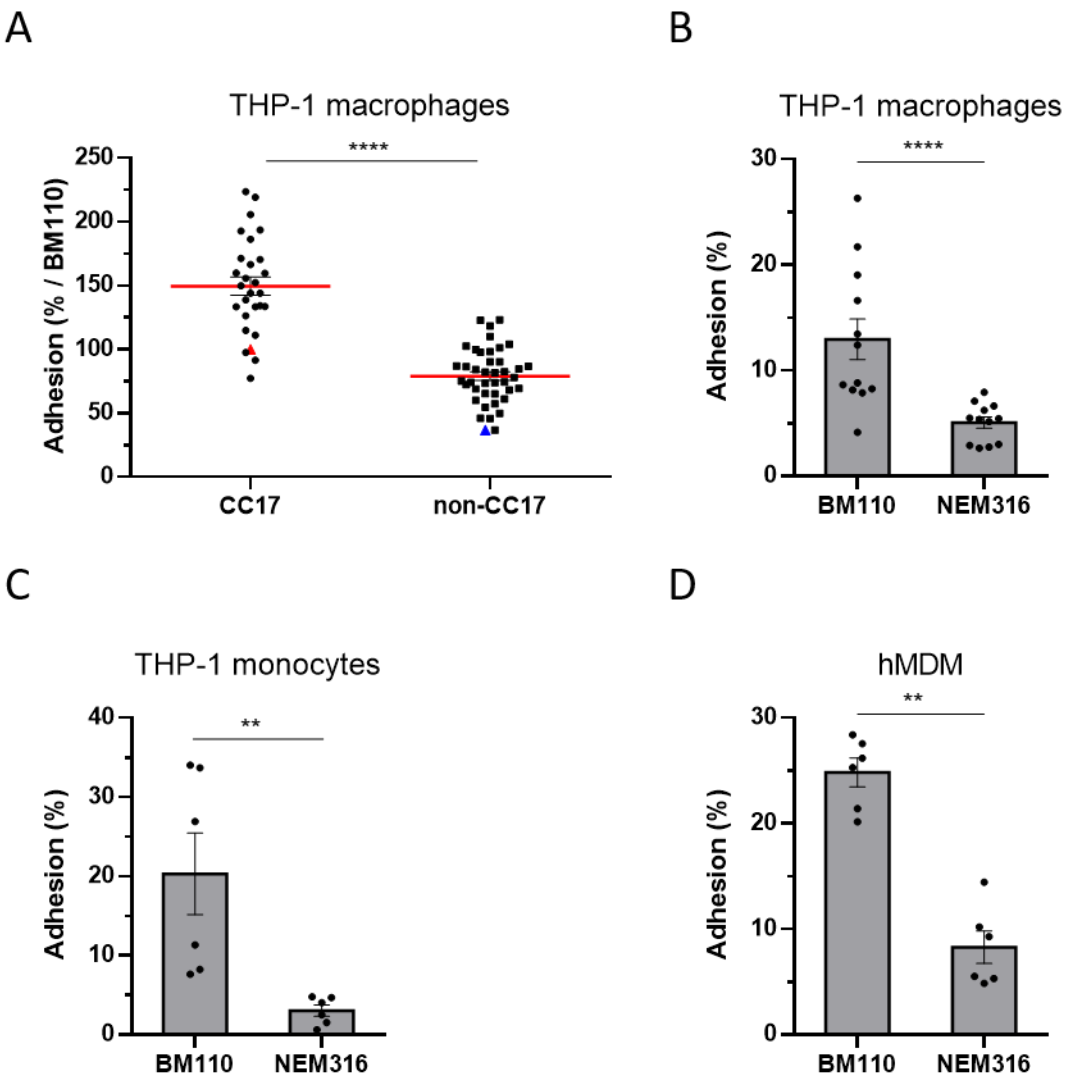

Figure 2: CC17 GBS strains are more adherent to phagocytes than non-CC17 strains. Adhesion level of GBS strains was assessed after one hour of infection at MOI 10, and at 4°C to avoid bacterial engulfment, by CFU counting using THP-1 cell line (A, B, C) or hMDM primary cells (D). Phagocytes were infected either with CC17 and non-CC17 GBS clinical isolates isolated from invasive infections, each point representing a clinical strain (A) or with GBS strains BM110 (CC17) and NEM316 (non-CC17) (B, C, D). Results are expressed as the percentage of adherent bacteria relative to the adhesion level of BM110 strain with the red horizontal lines indicating mean value (A) or to the initial inoculum (B, C, D). Statistical analysis: data shown are mean ± SEM of at least four independent experiments. Mann Whitney test (B, C, D) or t test (A) were performed with NS, non-significant; *, $p < 0.05$; **, $p < 0.01$; ***, $p < 0.001$.

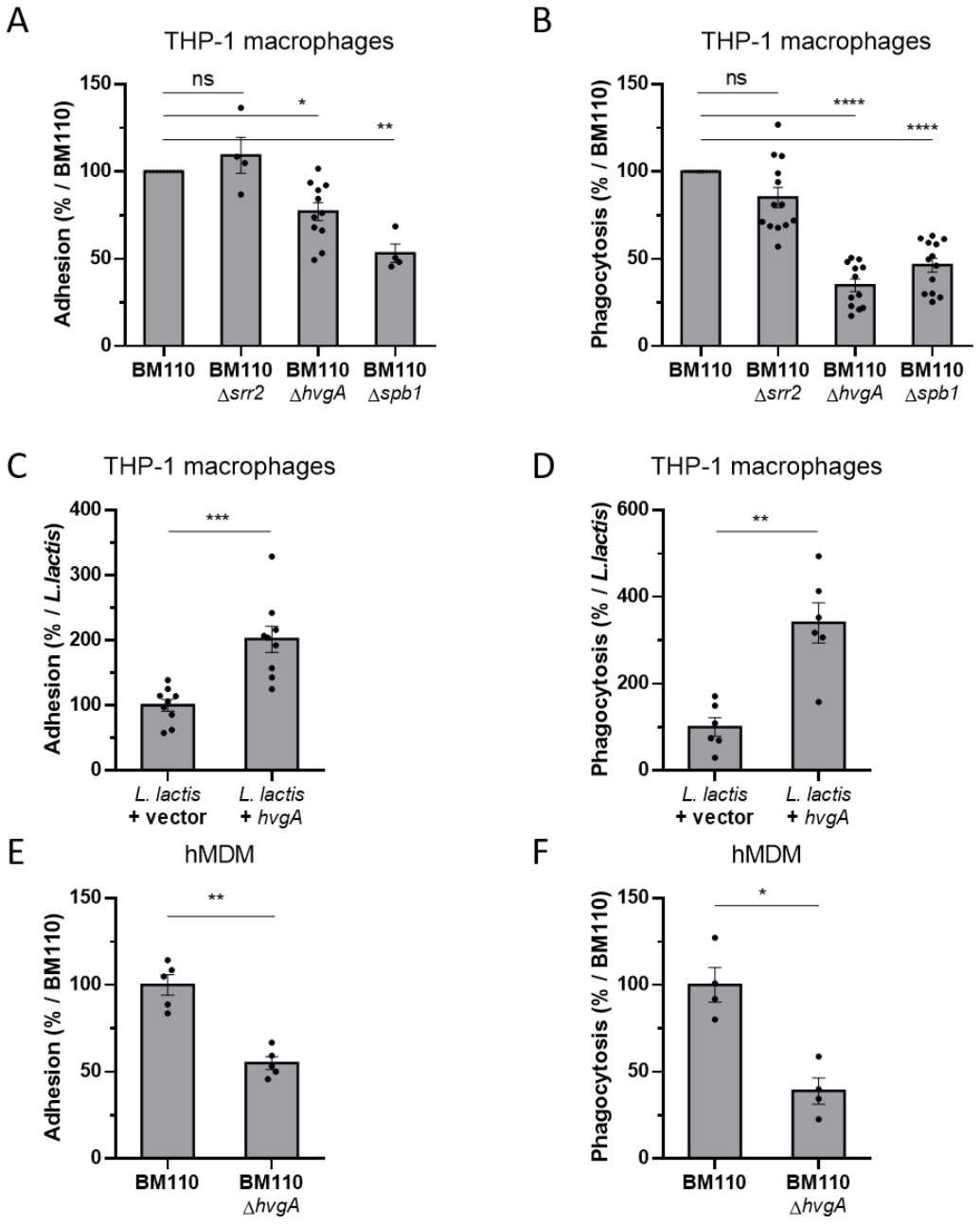

Figure 3: HvgA surface protein and Spb1 pilus protein are involved in CC17's hyper-adhesion and phagocytosis. Adhesion (A, C, E) and phagocytosis (B, D, F) levels were assessed using THP-1 macrophages cell line (A, B, C, D) or hMDM primary cells (E, F). Macrophages were infected with BM110 (CC17 strain) and its derivative mutated strains (BM110Δ*srr2*, BM110Δ*hvgA* or BM110Δ*spb1* (A, B, E, F), or with *Lactococcus lactis* strain carrying an empty vector (*L;lactis* + vector) or a vector expressing HvgA protein (*L. lactis* +HvgA) (C, D). Results are expressed as relative level compared to BM110 strain (A-F). Statistical analysis: data shown are mean ± SEM of at least four independent experiments. Kruskall Wallis test followed by Dunn's multiple comparisons tests (A, B), and Mann Whitney test (C, D, E, F), were performed, with NS, non-significant; *, $p < 0.05$; **, $p < 0.01$; ***, $p < 0.001$.

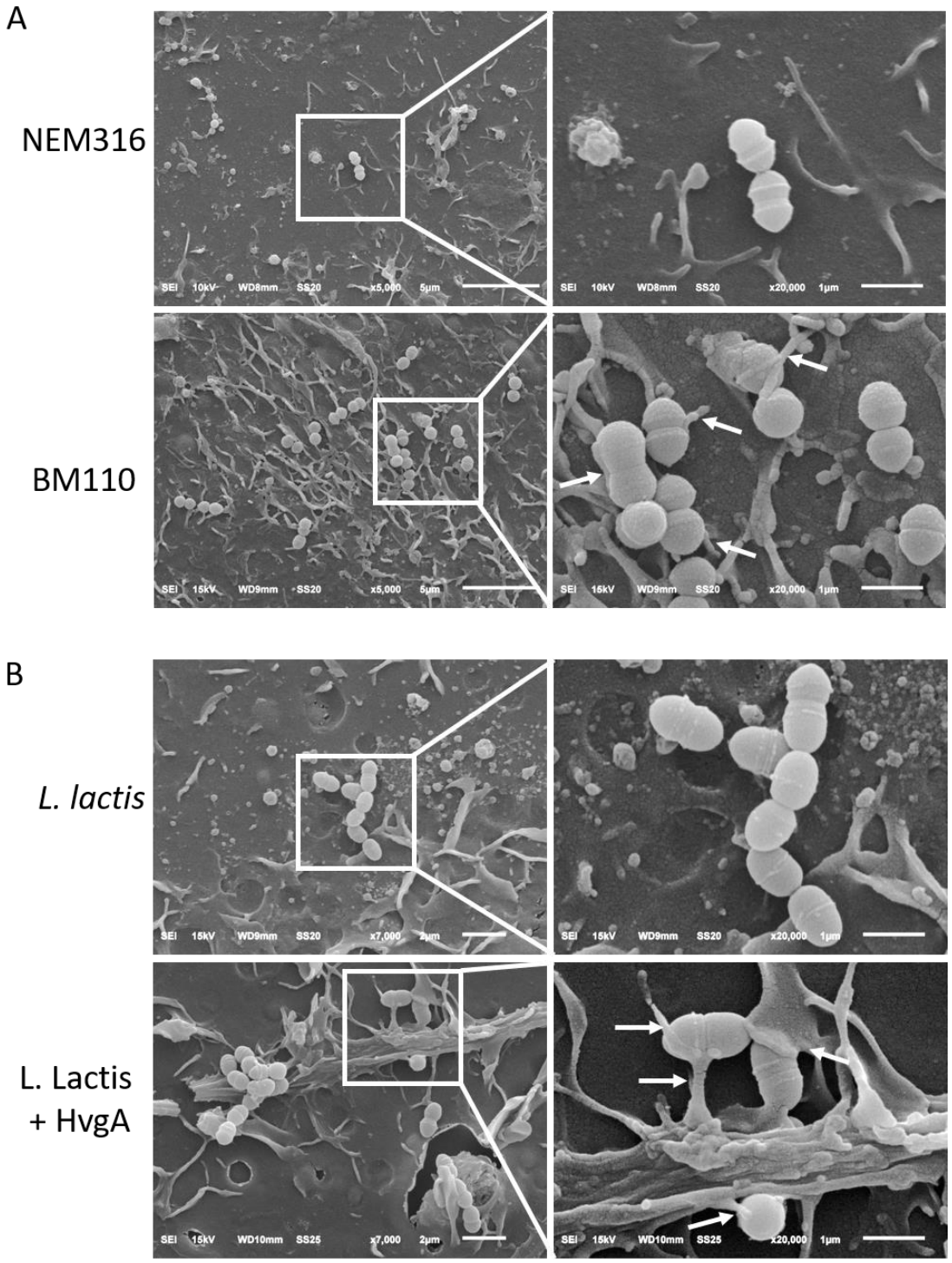

Fig 4: CC17 bacteria are captured by filopodia. Scanning electron microscopy (SEM) micrographs of THP-1 macrophages infected for 15 min (A) or 30 min (B). (A and B, left panel). Micrographs showing bacterial adherence to macrophages cell surface. Boxed areas correspond to magnification of insets (right panel) showing the capture of BM110 (CC17 strain) and *Lactococcus lactis* expressing HvgA (*L. lactis* +HvgA) by filopodia (arrows), while very few filopodia were observed for NEM316 and *L. lactis* strains.

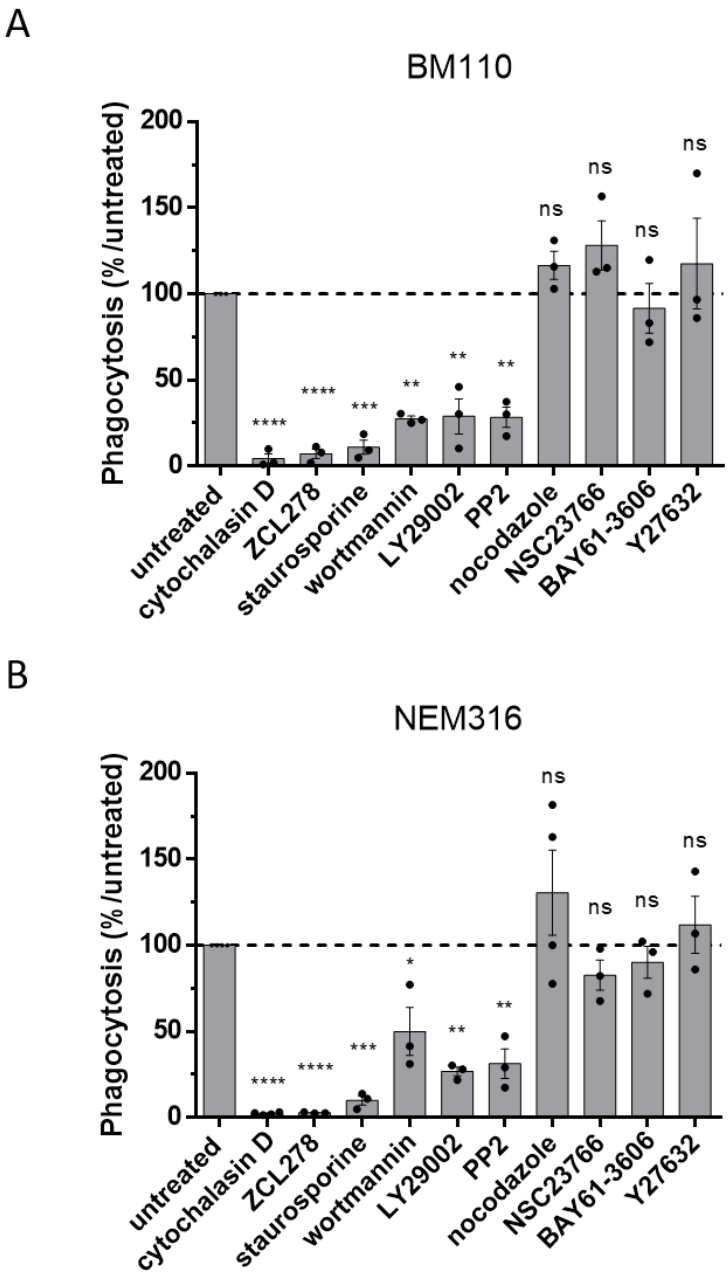

Fig 5: Signal transduction leading to phagocytosis is similar for CC17 and non-CC17 strains. Phagocytosis of BM110 (CC17 strain) (A) or NEM316 (non-CC17 strain) (B) were assessed by CFU counting after 45 min of infection at MOI 10 followed by 1h antibiotic treatment to kill extracellular bacteria using THP-1 macrophages. Cells were pre-treated for one-hour prior infection with cytochalasinD, ZCL178, staurosporin, wortmannin, LY29002, PP2, nocodazole, NSC23766, BAY61-3606 and Y27632 to inhibit actin polymerization, CDC42, protein kinase C, PI3kinase, Pi3kinase, Src kinase, microtubule polymerization, Rac, Syc and Rock, respectively. Results are expressed as the percentage of phagocytosis relative to untreated condition. Statistical analysis: data shown are mean ± SEM of at least four independent experiments. One-Way ANOVA with Dunnett multiple comparisons test were performed with NS, non-significant; *, $p < 0.05$; **, $p < 0.01$; ***, $p < 0.001$.

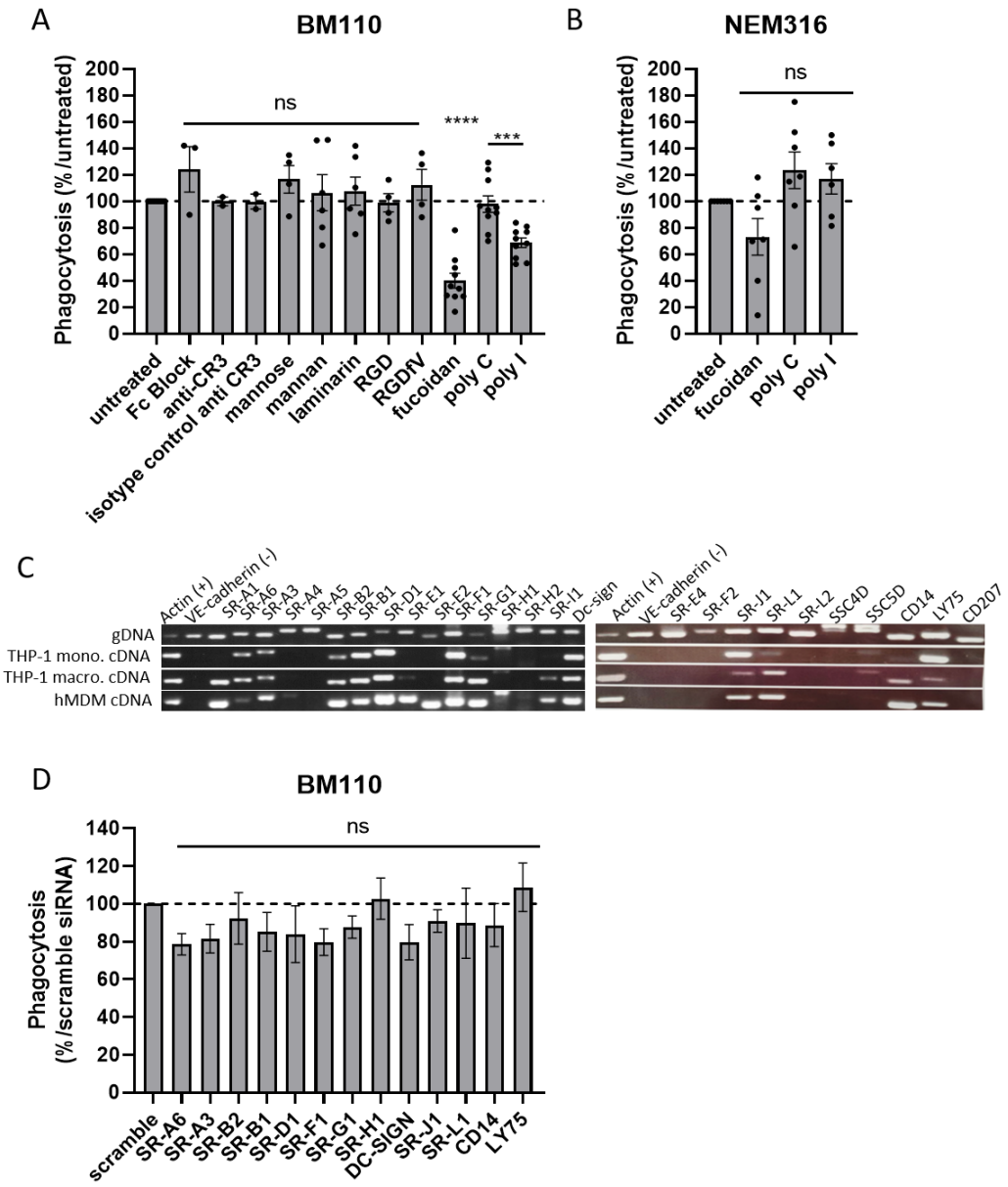

Fig 6: Scavenger receptors inhibitors leads to a decreased phagocytosis level of CC17 GBS in macrophages. (A, B, D) Phagocytosis level in THP-1 macrophages was assessed by CFU counting after 45 min of infection at MOI 10 with GBS strain BM110 (CC17 strain) (A, D) or NEM16 (non-CC17 strain) (B). followed by 1h antibiotic treatment to kill extracellular bacteria. (A) Macrophages were pre-treated 1h before infection to block FCγ receptors (Fc Block™), complement receptor 3 (CR3 blocking antibody), lectin receptors (mannose, mannan, laminarin), integrins receptors (RGD and RGDfV mimetic peptides), or (A, B) scavenger receptors inhibitors (Fucoidan and poly(I) or inactive analog poly(C). (C) Expression of scavenger receptors genes was assessed by RT-PCR using THP-1 macrophages, THP-1 monocyte and hMDM cDNA. Actin and VE-cadherin gene expression was used as positive and negative controls of expression, respectively. Genomic DNA (gDNA) was used to validate primers efficiency. (D) Involvement of scavenger receptors on BM110 (CC17 strain) phagocytosis was assessed by silencing scavenger receptors expression

by si-RNA screening. Results are expressed as the percentage of phagocytosis relative to the untreated control condition (A, B) or to the scramble control condition (D). Statistical analysis: data shown are mean ± SEM of at least four independent experiments. Kruskall Wallis test followed by Dunn's multiple comparisons tests were performed (A, B, D), with NS, non-significant; *, $p < 0.05$; **, $p < 0.01$; ***, $p < 0.001$.

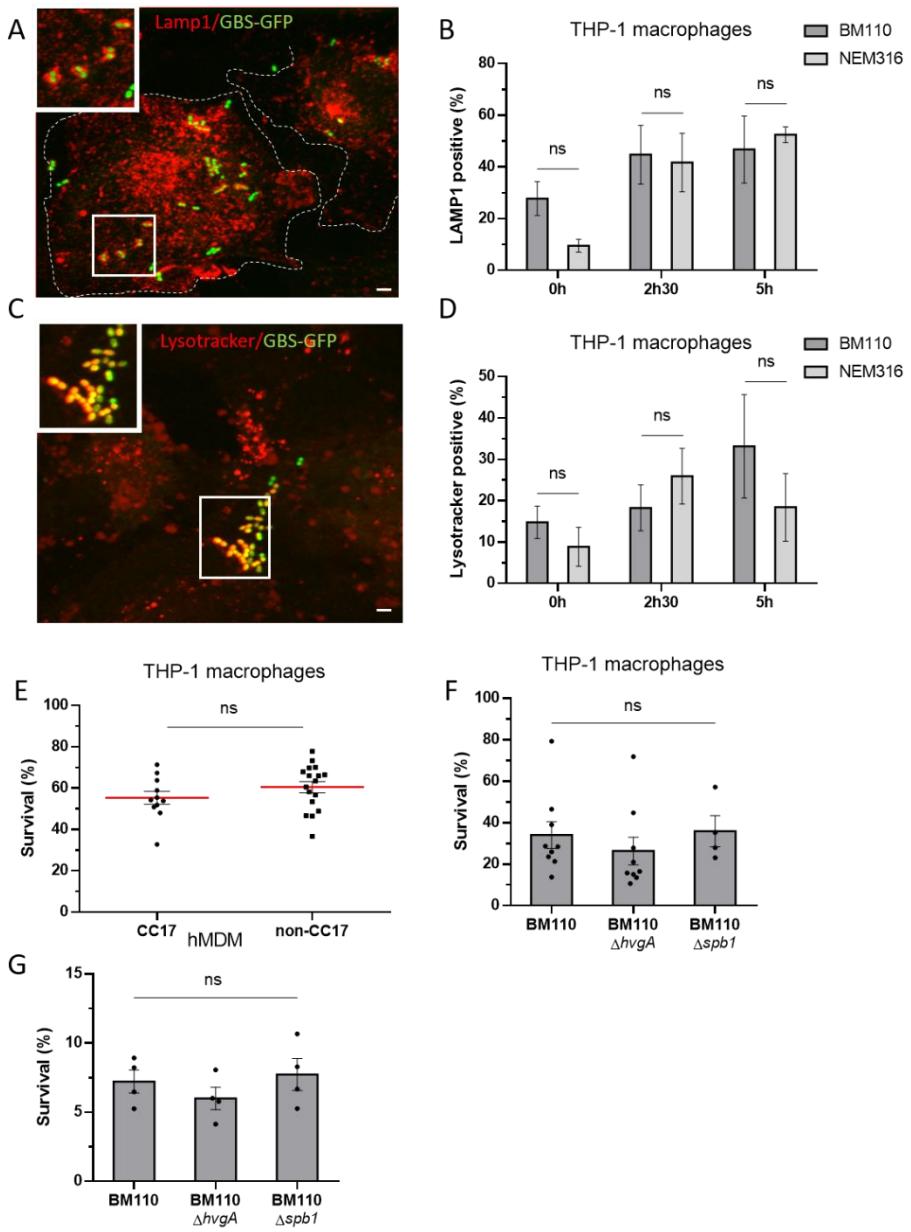

Figure 7: CC17 and non-CC17 GBS strains exhibit similar intracellular fate. Intracellular fate of BM110 (CC17) and NEM316 (non-CC17) strains was followed by microscopy (A, D) or CFU count (E, F, G) in THP-1 macrophages (A, F) or hMDM (G). (A, C) Representative confocal microscopy images of THP-1 macrophages infected with BM110-GFP (CC17 strain) (green) and labelled with anti-LAMP1 antibody (red) (A) or Lysotracker® (red) (B). Boxed areas correspond to magnification of insets. Dotted lines indicate cell perimeters. Scale bar: 5 µm. (B, D) Quantification of bacteria associated with LAMP1 (B) or Lysotracker® (D) was performed after 0, 2h30 or 5 h post-phagocytosis. Results are expressed as the percentage of bacteria positive for LAMP1 (B) or Lysotracker® (D) staining. (E, F, G) Percentage of survival was assessed by CFU counting of viable bacteria 2h30 after phagocytosis. (E) Macrophages were infected with CC17 and non-CC17 GBS clinical isolates from invasive infections, each point representing a clinical strain or (F, G) with the BM110 (CC17) strain and its derivative mutated strains (BM110Δ*hvgA* or BM110Δ*spb1*). Results

are expressed as the percentage of viable intracellular bacteria normalized to the initial phagocytosis level intracellular load. Statistical analysis: data shown are mean ± SEM of at least four independent experiments. (E) Two-way ANOVA (A), Tuckey multiple comparison (B, D) and Mann Whitney (E, F, G) tests were performed with NS, non-significant; *, $p < 0.05$; **, $p < 0.01$; ***, $p < 0.001$.

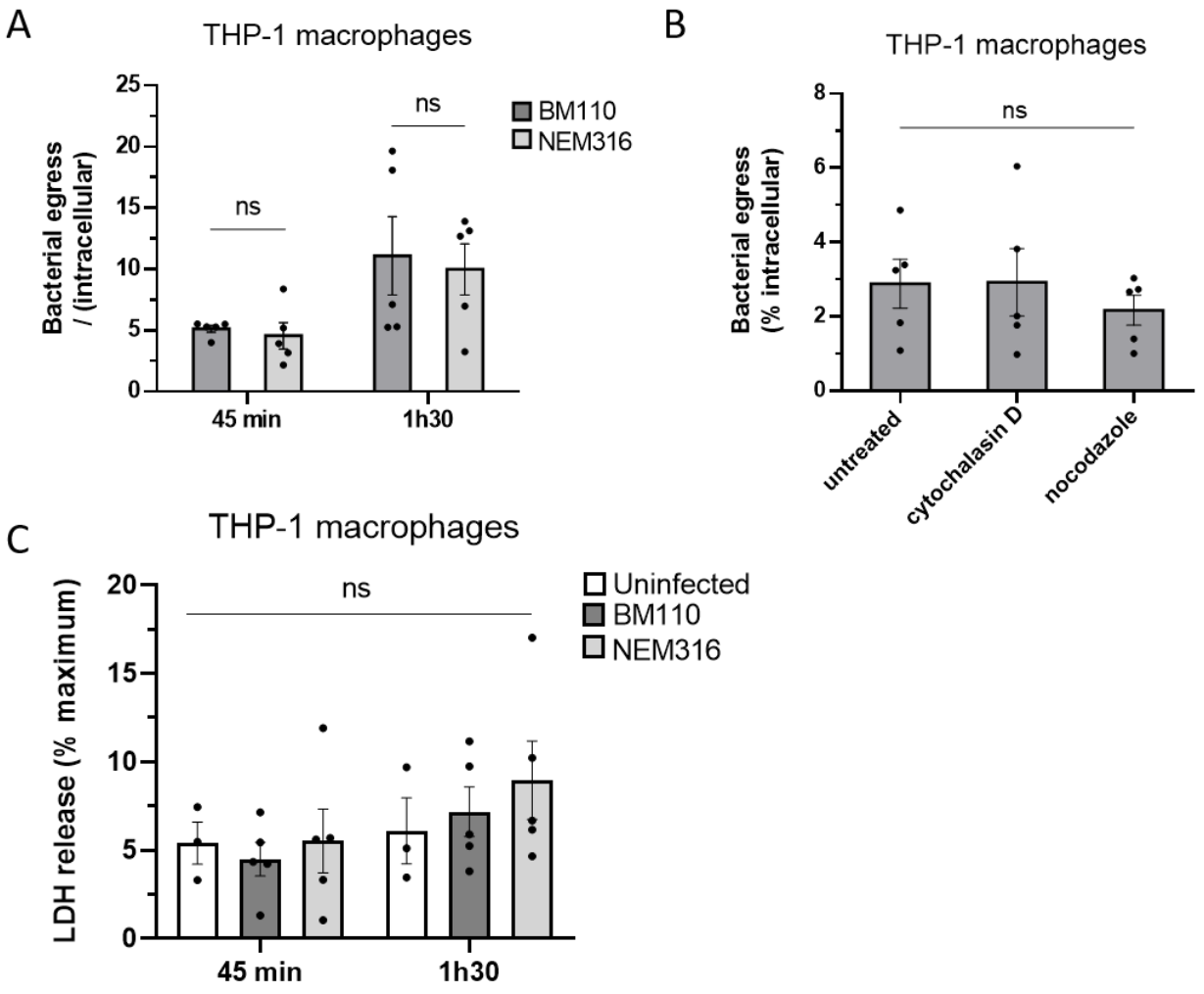

Fig 8: GBS strains can escape macrophages independently of actin and microtubules. GBS egress from THP-1 macrophages was assessed by CFU counting. THP-1 were infected for 45 min or 1h30 at MOI 10 with GBS strains, then treated with antibiotic to kill extracellular bacteria. Bacterial egress was measured for BM110 (CC17) or NEM316 (non-CC17) strains in absence of any treatment (A) or in the presence of actin (cytochalasin D) or microtubules (nocodazole) depolymerizing agents added after phagocytosis (B). Results are expressed as the percentage of viable bacteria release in the cell supernatants normalized to the number of phagocytosed bacteria (A, B). Cell lysis during bacterial egress was measured by evaluating LDH release (C). Statistical analysis: data shown are mean ± SEM of at least four independent experiments. Two-way Anova with Bonferroni post-test (A) Kruskall Wallis (B) and one-Way ANOVA with Dunnett's post-tests were performed with NS, non-significant; *, $p < 0.05$; **, $p < 0.01$; ***, $p < 0.001$.

SUPPLEMENTARY

TABLE S1: Bacterial strains used in this study.

Strains	Relevant characteristics	Reference
BM110	serotype III, CC17, bacteremia	(49)
BM110-GFP	BM110 strain carrying pGU2664plasmid for GFP expression	(17)
BM110 Δ*srr2*	BM110 strain deleted in *srr2* gene	(8)
BM110 Δ*hvgA*	BM110 strain deleted in *hvgA*gene	(16)
BM110 Δ*spb1*	BM110 strain deleted in spb1 gene	(27)
BM110 Δ*cps*	BM110 strain deleted in *cps*D/E genes (capsular mutant)	(50)
NEM316	serotype III, CC23, EOD bacteremia	(16)
NEM316-GFP	NEM316 strain carrying pGU2664plasmid for GFP expression	This study
NEM316 Δ*cps*	NEM316 strain deleted in gene (capsule mutant)	(50)
L. lactis-pOri232	MG1363 strain of *Lactococcus lactis* subsp. *cremoris* carrying empty pOri232 plasmid	(16)
L. lactis-P*hvgA*	MG1363 strain carrying pOri232 plasmid for HvgA expression	(16)

TABLE S2: GBS clinical isolates used in this study.

Strains	Capsular serotype	Complex clonal (CC)	Type of infection
CNR CCH1569	CPS III	CC17	LOD Meningitis
CNR CCH1570	CPS III	CC17	LOD Meningitis
CNR CCH1571	CPS III	CC17	LOD Meningitis
CNR CCH1573	CPS III	CC17	LOD Bacteremia
CNR CCH1575	CPS III	CC17	LOD Meningitis
CNR CCH1577	CPS III	CC17	EOD Meningitis
CNR CCH1578	CPS III	CC17	LOD Meningitis
CNR CCH1581	CPS III	CC17	EOD Meningitis
CNR CCH1584	CPS III	CC17	LOD Meningitis
CNR CCH1586	CPS III	CC17	LOD Meningitis
CNR CCH1588	CPS III	CC17	LOD Meningitis
CNR CCH1589	CPS III	CC17	LOD Meningitis
CNR CCH1591	CPS III	CC17	LOD Meningitis
CNR CCH1594	CPS III	CC17	LOD Meningitis
CNR CCH1596	CPS III	CC17	LOD Meningitis
CNR CCH1597	CPS III	CC17	LOD Meningitis
CNR CCH1602	CPS III	CC17	EOD Meningitis
CNR CCH0620	CPS IV	CC17	Adult Bacteremia
CNR CCH0755	CPS IV	CC17	Adult Bacteremia
CNR CCH0778	CPS IV	CC17	Adult Bacteremia
CNR CCH0950	CPS IV	CC17	Adult Bacteremia
CNR CCH1030	CPS IV	CC17	Adult Meningitis
CNR CCH1174	CPS IV	CC17	Adult Bacteremia
CNR CCH1239	CPS IV	CC17	Adult Bacteremia
CNR CCH1360	CPS IV	CC17	Adult Meningitis
CNR CCH1472	CPS IV	CC17	EOD pneumonia
CNR CCH1506	CPS IV	CC17	LOD Bacteremia
CNR CCH0050	CPS III	non-CC17	EOD Bacteremia
CNR CCH0107	CPS III	non-CC17	LOD Meningitis
CNR CCH0112	CPS III	non-CC17	EOD Bacteremia
CNR CCH0150	CPS III	non-CC17	LOD Bacteremia
CNR CCH0205	CPS III	non-CC17	LOD Bacteremia
CNR CCH0311	CPS III	non-CC17	EOD Bacteremia
CNR CCH0362	CPS III	non-CC17	LOD Bacteremia
CNR CCH0382	CPS III	non-CC17	Adult osteoarticular infection
CNR CCH0384	CPS III	non-CC17	LOD Bacteremia
CNR CCH0513	CPS III	non-CC17	LOD Meningitis
CNR CCH0700	CPS III	non-CC17	LOD Meningitis
CNR CCH1207	CPS III	non-CC17	LOD Meningitis
CNR CCH1261	CPS III	non-CC17	LOD Bacteremia
CNR CCH1280	CPS III	non-CC17	LOD Meningitis
CNR CCH1319	CPS III	non-CC17	LOD Bacteremia
CNR CCH1393	CPS III	non-CC17	LOD Bacteremia
CNR CCH1396	CPS III	non-CC17	LOD Bacteremia

CNR CCH1490	CPS III	non-CC17	Intra-uterine infection (pregnancy-associated)
CNR CCH1809	CPS III	non-CC17	LOD Bacteremia
CNR CCH1881	CPS III	non-CC17	LOD Meningitis
CNR CCH1585	CPS IV	non-CC17	EOD Bacteremia
CNR CCH0966	CPS IV	non-CC17	EOD Meningitis
CNR CCH1134	CPS IV	non-CC17	Adult Bacteremia
CNR CCH1157	CPS IV	non-CC17	LOD pneumonia
CNR CCH1165	CPS IV	non-CC17	EOD Bacteremia
CNR CCH1274	CPS IV	non-CC17	Adult Bacteremia
CNR CCH1363	CPS IV	non-CC17	LOD Bacteremia
CNR CCH1369	CPS IV	non-CC17	Adult Bacteremia
CNR CCH1403	CPS IV	non-CC17	Adult Bacteremia
CNR CCH1686	CPS IV	non-CC17	LOD Bacteremia
CNR CCH1565	CPS II	non-CC17	EOD Bacteremia
CNR CCH1566	CPS Ia	non-CC17	EOD Meningitis
CNR CCH1567	CPS Ia	non-CC17	EOD Bacteremia
CNR CCH1568	CPS Ia	non-CC17	EOD Bacteremia
CNR CCH1572	CPS Ia	non-CC17	EOD Bacteremia
CNR CCH1576	CPS Ia	non-CC17	EOD Bacteremia
CNR CCH1579	CPS V	non-CC17	EOD Bacteremia
CNR CCH1580	CPS V	non-CC17	LOD Bacteremia
CNR CCH1582	CPS Ib	non-CC17	LOD Meningitis
CNR CCH1583	CPS Ia	non-CC17	LOD Bacteremia

TABLE S3: Inhibitors used in this study.

Chemical and reagents	Target	Concentration
Cytochalasine D	Actin filaments	2 µM
Nocodazole	Microtubules	1 µM
Wortmannin	Pi 3-kinase	100 nM
LY29002	Pi 3-kinase	40 µM
PP2	Src kinase	10 µM
Staurosporin	Protein kinase C	500 nM
NSC23766	Rac	100 µM
ZCL278	CDC42	50 µM
Bay61-3606	Syk	1 µM
Y27632	Rock	10 µM
Human FC Block™	FCy receptors	2 µg/ml
Vim12 antibody	Complement Receptor 3	20 µg/ml
IgG1 mouse antibody	Isotype control	20 µg/ml
Mannan	Lectin receptors	200 µg/ml
Mannose	Lectin receptors	1%
Laminarin	Lectin receptors	200 µg/ml
RGD peptide	RGD dependent integrins	50 µM
RGDfV	RGDfV dependent integrins	50 µM
Fucoidan	Scavenger receptors	500 µg/ml
Poly (I)	Scavenger receptors	200 µg/ml
Poly (C)	Inactive analog of Poly(I)	200 µg/ml

TABLE S4: Primers used in this study.

Target	Primers	Sequence (5'-3')	Expected size (bp)
Actin	F-1462 R-1580	TTCCAAATATGAGATGCGTTGTTA ATGCTATCACCTCCCCTGTG	118
VE-cadherin	F-453 R-571	GGTCGATGCAGAGACAGGAG GAGTCTCCAGGTTTTCGCCA	118
SR-A1/MSR1	F-595 R-707	GCCAACCTCATGGACACAGA CCATGTCCCTGGACTGAGGA	112
SR-A6/MARCO	F-1228 R-1361	TGTGGAGCTGCACCAAGAAT CCACATATGAGCCCGAGGAC	133
SR-A3/SCARA3	F-866 R-992	CGAGGAGACCCTGACCCTCCAG CCCAGGGTGGCCTGGATGTTC	126
SR-A4/SCARA4	F-618 R-796	ACGCTGGAGAAGTTACAGGC TTCTGCAGATTGCCCTGGAG	178
SR-A5/SCARA5	F-2386 R-2579	CCATGCACCAGGCCTCAATA CACTTGACGTTGCCTCTTGC	193
SR-B2/CD36	F-1559 R-1682	CAATTTGCAAAACGGCTGCAG CTTCTCATCACCAATGGTCCC	123
SR-B1/SCARB1	F-1520 R-1652	AGGGGGAGACTCTTCACACA GGCTCCGGATTTGGCAGATG	132
SR-D1/CD68	F-1093 R-1261	GATCCTTCTTGGCCTCCTCG CTTTGAGCCAGTTGCGTGTC	168
SR-E1/LOX1	F-740 R-920	CGAGGAGCTGTTTATGCGGA TGGCACCCAAGTGACAAAGA	180
SR-E2/Dectin1	F-830 R-943	ACCCATCTCCAAATTGTGTA CCACCCTTCCTCTTACATTG	113
SR-F1/SCARF1	F-2964 R-3100	CTCCCTCTGTCCCCCAGGCT GCCAAGCGTGGTGGAGGGCACC	136
SR-G1/CXCL16	F-1041 R-1162	CCACCCTCCCAGTAGGATCA CTGCTTCTGGTTCTCCCCAG	121
SR-H1/FEEL1	F-774 R-937	CAACCCCTGCTGGCCATCAC GTAGAGTTGCTGGGGCAGCC	163
SR-H2/FEEL2	F-4194 R-4375	GCTGTGCCGGCTTCTTTGGC GGTCACAGTGGATGCCGTAC	181
SR-I1/CD163	F-310 R-455	GCGGGAGAGTGGAAGTGAAA ACCTGCACTGGAATTAGCCC	145
SR-J1/RAGE	F-1431 R-1571	GGCCCACAGACAGATCCCAT GGGGGCTCTGGTTGTAGAAG	140
SR-E4/ASGPR	F-155 R-289	GGAATCAGACCCTGAGACCC TGCAGCTGGGAGTCTTTTCTG	134
SR-F2/MEGF10	F-29 R-177	AGCAAGTACTTTCCCGGTGC CAATCAACGCGGTTAGCGTC	148
SR-L1/LRP1	F-3616 R-3770	GACTGTGGGGACAACAGTGAC TTGGCGTGTGTCTCATCACT	154
SR-L2/LRP2	F-15028	AGCCTCAACTGGGTTTTTGT	129

	R-15157	GTACACATTTAGCCACAGGGC	
SSC4D/SRCRB4D	F-2046 R-2228	GGACAATGTCAAGTGCCGTGGG GTAGTCATCACAAGAGGAGGGC	182
SSC5D	F-1990 R-2160	CTGGAGAAAACAACCACGAAG GTCAGTGCTGCAGTGGTCTGTG	170
CD14	F-352 R-466	CTGACACGGTCAAGGCTCTC AGTTCCTTGAGGCGGGAGTA	114
LY75	F-5058 R-5185	ACTGATGAGAAACCCGCCAG ACTGATGAGAAACCCGCCAG	127
CD207/Langerin	F-963 R-1066	ATGCCCCATGTGACAAAACG GCGTTGGAGCTCAAAGAGTG	103

Figure S1: GBS Capsule is not involved the hyper phagocytosis of CC17 strains. Phagocytosis level of GBS strains was assessed by CFU counting after 45 min of infection at MOI 10 followed by 1h antibiotic treatment to kill extracellular bacteria, using THP-1 cell line. THP-1 macrophages were infected with (A) CC17 and non-CC17 GBS clinical isolates from invasive infections. Each point represents a clinical strain. Results are shown according to capsular type (CPS III, CPS IV, or other CPS) or (B) with GBS strain BM1110 (CC17) and NEM316 (non-CC17) strains and their respective mutant impaired for capsule expression. (A, B) Results are expressed as the percentage of phagocytosis relative to BM110 phagocytosis (A), or as a percentage of the bacterial initial inoculum (B). Statistical analysis: data shown are mean ± SEM of at least four independent experiments. Two-way ANOVA (A, B) were performed with NS, non-significant; *, $p < 0.05$; **, $p < 0.01$; ***, $p < 0.001$.

Figure S2: GBS Capsule is not involved the hyper-adhesion of CC17 strains. Adhesion level of GBS strains was assessed by CFU counting after 45 min of infection at MOI 10 and at 4°C to avoid bacterial engulfment, using THP-1 cell line. THP-1 macrophages were infected with (A) CC17 and non-CC17 GBS clinical isolates from invasive infections. Each point represents a clinical strain. Results are shown according to capsular type (CPS III, CPS IV, or other CPS) or (B) with GBS strain BM1110 (CC17) and NEM316 (non-CC17) strains impaired for capsule expression. (A) Results are expressed as relative level compared to BM110 reference strain or (B) as a percentage of the bacterial initial inoculum. Statistical analysis: data shown are mean ± SEM of at least four independent experiments. Two-way ANOVA (A) or Mann Whitney test (B) were performed with NS, non-significant; *, $p < 0.05$; **, $p < 0.01$; ***, $p < 0.001$.

Figure S3: siRNA screen in THP-1 macrophages. Figure S3: siRNA screen in THP-1 macrophages. (A) Silencing efficiency obtained by siRNA treatment of THP-1 macrophages was evaluated by western blot analysis on 2 independent targets (integrin α5 and β3) (B) Phagocytosis of complement-opsonized red

blood cells was evaluated my fluorescence microscopy in THP-1 treated with scramble siRNA or siRNA targeting complement receptors (CR, *itgαM*). Results are expressed as the percentage of phagocytosed red blood cells normalized to scramble control condition. (C) Phagocytosis of BM110 (CC17) strain was evaluated THP-1 macrophages treated with siRNA targeting FCγR1; FCγR2A,B,C; complement receptor (CR, *itgAM*), PLAUR, SR-K1 (CD44) and integrins α5 and β3. Results are expressed as the percentage of phagocytosis normalised to scramble control conditions. Statistical analysis: data shown are mean ± SEM. One-way ANOVA (C) was performed with NS, non-significant; *, $p < 0.05$; **, $p < 0.01$; ***, $p < 0.001$.

Figure S4: Survival of GBS strains is independent of capsular serotype. Survival level of GBS strains in THP-1 macrophages was assessed by CFU counting 2 hrs post-phagocytosis. THP-1 macrophages were infected with CC17 and non-CC17 GBS clinical isolates from invasive infections. Each point represents a clinical strain. Results are shown according to capsular type (CPS III, CPS IV, or another CPS). Results are expressed as the percentage of viable intracellular bacteria normalized to the number of phagocytosed bacteria. Statistical analysis: data shown are mean ± SEM of at least four independent experiments. Two-way ANOVA was performed with NS, non-significant; *, $p < 0.05$; **, $p < 0.01$; ***, $p < 0.001$.

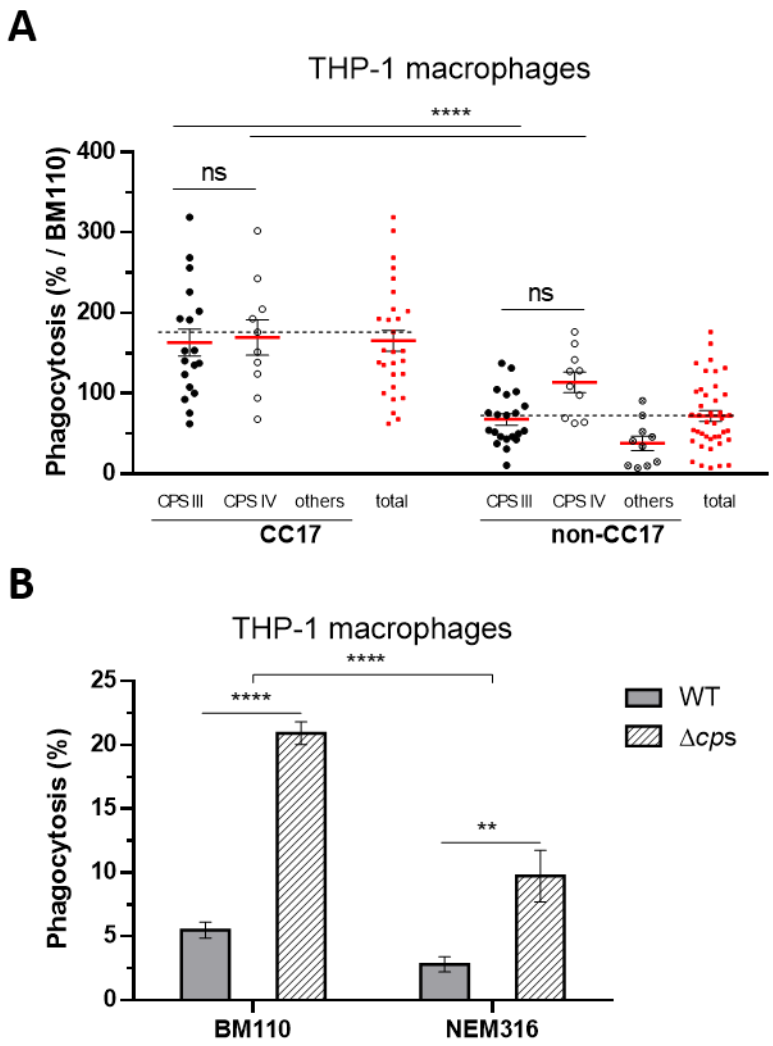

Figure S1: GBS Capsule is not involved the hyper phagocytosis of CC17 strains. Phagocytosis level of GBS strains was assessed by CFU counting after 45 min of infection at MOI 10 followed by 1h antibiotic treatment to kill extracellular bacteria, using THP-1 cell line. THP-1 macrophages were infected with (A) CC17 and non-CC17 GBS clinical isolates from invasive infections. Each point represents a clinical strain. Results are shown according to capsular type (CPS III, CPS IV, or other CPS) or (B) with GBS strain BM1110 (CC17) and NEM316 (non-CC17) strains and their respective mutant impaired for capsule expression. (A, B) Results are expressed as the percentage of phagocytosis relative to BM110 phagocytosis (A), or as a percentage of the bacterial initial inoculum (B). Statistical analysis: data shown are mean ± SEM of at least four independent experiments. Two-way ANOVA (A, B) were performed with NS, non-significant; *, $p < 0.05$; **, $p < 0.01$; ***, $p < 0.001$.

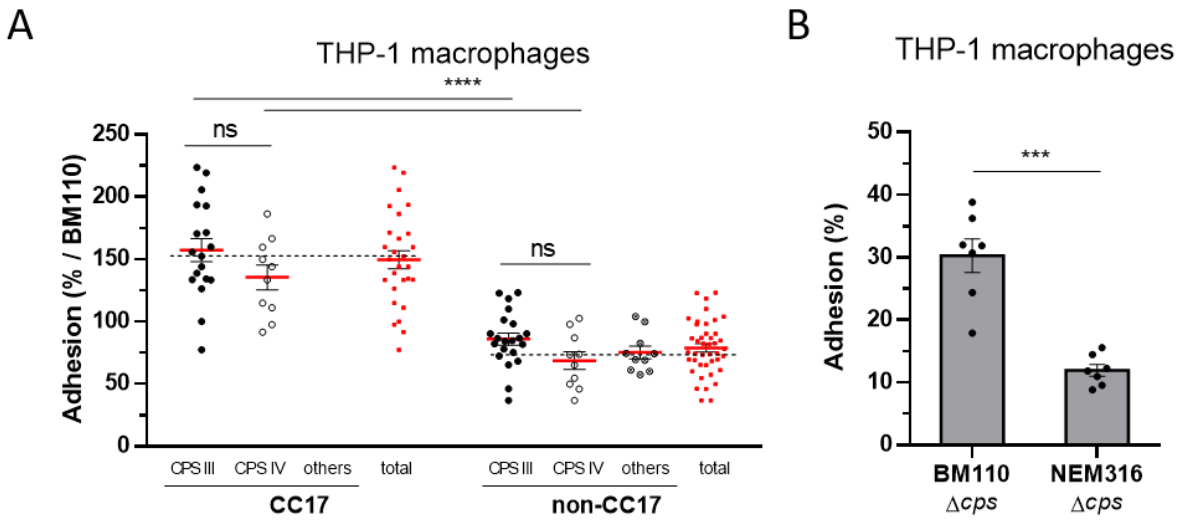

Figure S2: GBS Capsule is not involved the hyper-adhesion of CC17 strains. Adhesion level of GBS strains was assessed by CFU counting after 45 min of infection at MOI 10 and at 4°C to avoid bacterial engulfment, using THP-1 cell line. THP-1 macrophages were infected with (A) CC17 and non-CC17 GBS clinical isolates from invasive infections. Each point represents a clinical strain. Results are shown according to capsular type (CPS III, CPS IV, or other CPS) or (B) with GBS strain BM1110 (CC17) and NEM316 (non-CC17) strains impaired for capsule expression. (A) Results are expressed as relative level compared to BM110 reference strain or (B) as a percentage of the bacterial initial inoculum. Statistical analysis: data shown are mean ± SEM of at least four independent experiments. Two-way ANOVA (A) or Mann Whitney test (B) were performed with NS, non-significant; *, $p < 0.05$; **, $p < 0.01$; ***, $p < 0.001$.

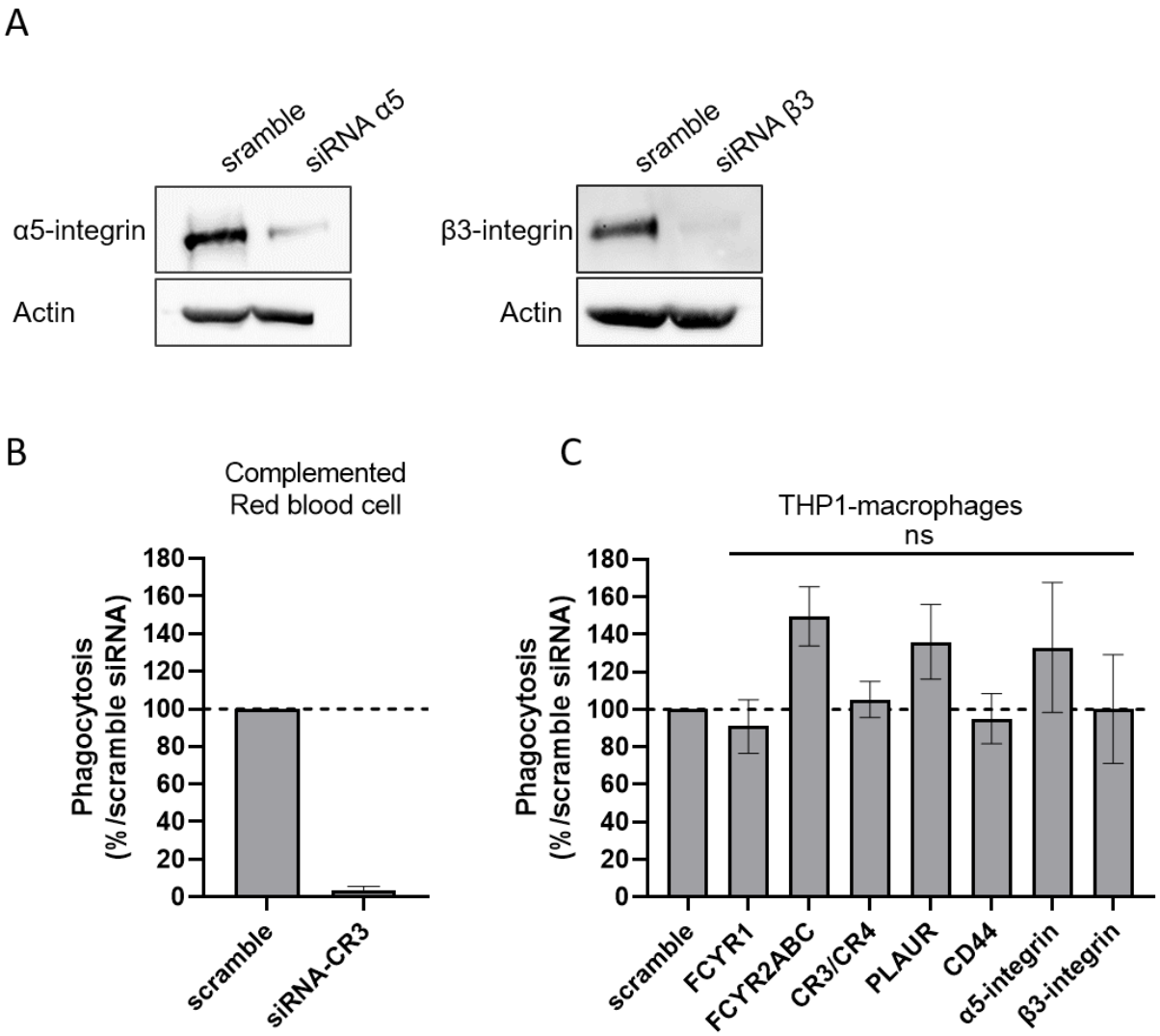

Figure S3: siRNA screen in THP-1 macrophages. (A) Silencing efficiency obtained by siRNA treatment of THP-1 macrophages was evaluated by western blot analysis on 2 independent targets (integrin α5 and β3) (B) Phagocytosis of complement-opsonized red blood cells was evaluated my fluorescence microscopy in THP-1 treated with scramble siRNA or siRNA targeting complement receptors (CR, *itgaM*). Results are expressed as the percentage of phagocytosed red blood cells normalized to scramble control condition. (C) Phagocytosis of BM110 (CC17) strain was evaluated THP-1 macrophages treated with siRNA targeting FCγR1; FCγR2A,B,C; complement receptor (CR, *itgAM*), PLAUR, SR-K1 (CD44) and integrins α5 and β3. Results are expressed as the percentage of phagocytosis normalised to scramble control conditions. Statistical analysis: data shown are mean ± SEM. One-way ANOVA (C) was performed with NS, non-significant; *, $p < 0.05$; **, $p < 0.01$; ***, $p < 0.001$.

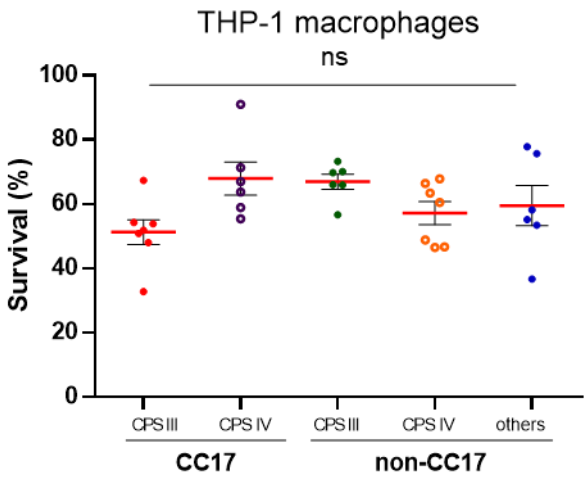

Figure S4: Survival of GBS strains is independent of capsular serotype. Survival level of GBS strains in THP-1 macrophages was assessed by CFU counting 2 hrs post-phagocytosis. THP-1 macrophages were infected with CC17 and non-CC17 GBS clinical isolates from invasive infections. Each point represents a clinical strain. Results are shown according to capsular type (CPS III, CPS IV, or another CPS). Results are expressed as the percentage of viable intracellular bacteria normalized to the number of phagocytosed bacteria. Statistical analysis: data shown are mean ± SEM of at least four independent experiments. Two-way ANOVA was performed with NS, non-significant; *, $p < 0.05$; **, $p < 0.01$; ***, $p < 0.001$.